INHIBITION OF HOST INNATE IMMUNE RESPONSES THROUGH THE MODULATION OF CYTOPLASMIC STRESS GRANULES BY ENCEPHALOMYOCARDITIS VIRUS PROTEASE

NG CHEN SENG

ABSTRACT

Cells initiate a series of signaling reprogramming in response to various environmental cues. In response of stress, cells initiate series of rapid changes, induce the aggregation of ribonucleoproteins, triggering the arrest of protein translation and disassembly of polysomes. Arrested RNA transcripts will be compartmentalized in a dense, non-membranous transient structure known as stress granule (SG). Viral infection also induces SG-like aggregation and the functional role of this structure still obscure. In our previously report, we demonstrated that SG is essential for inducing type I IFN in response to IAVΔNS1 infection in a PKR-dependent manner, and expression of NS1 protein impaired SG formation, as well as IFN-induction. In this study, I further investigated SG formation by various types of RNA and DNA viruses. I established an imaging system by using Ras-GAP SH3 domain binding protein-1 (G3BP1) as an SG probe, for real-time monitoring of virus-induced SG (vSG). Cells infected with RNA and DNA viruses predominantly displayed four distinct types of formation patterns: stable formation, transient formation, alternate formation, and no formation. I further investigated the role of SGs in response to Encephalomyocarditis virus (EMCV) infection, SGs tend to form but dispersed at the later stage of infection due to cleavage by EMCV protein 3C protease. Expression of cleavage resistant G3BP1 succeeds in restoring the stable formation of SG. EMCV-induced SG formation is also mediated through PKR pathway. Interestingly, cleavage resistant G3BP1 enhance MDA5-induced type I interferon production at the later stage of infection. I further showed that siRNA knockdown of endogenous G3BP1 also impaired the activation of IFN-β gene and other chemokines, and hence potentiates viral replication. IFN-induction at the initial time point was not affected in both EGFP-G3BP1 wild-type and siRNA depletion system, highlighting the critical role of SG in EMCV-induced IFN response at the later time phase. My findings suggest the indispensable role of SGs as an antiviral platform and define the mechanism on how viral proteins interfere with host antiviral responses.

TABLE OF CONTENTS

LIST OF SYMBOLS, UNITS AND ABBREVIATION

G	glycine
Q	glutamine
D	aspartic acid
R	arginine
Y	tyrosine
A	alanine
K	lysine
T	threonine
C	cysteine
S	serine
F	phenylalanine
I	isoleucine
w/v	weight over volume
v/v	volume over volume
%	percent
s	second
ml	mililiter
μl	microliter
ºC	degree Celcius
r.p.m	rotation per minute
M	Molar
mM	miliMolar
μM	microMolar
mm	millimeter
mg/ml	milligram per milliliter
min	minute
IFN	interferon
PCR	polymerase chain reaction
dNTP	deoxynucleotides-triphosphate
NaOH	sodium hydroxide

HCl	hydrochloride
BSA	bovine serum albumin
FBS	foetal bovine serum
vSG	virus-induced stress granules
DNA	deoxyribonucleic acid
PBS	phosphate-buffer-saline
PBST	phosphate-buffer-saline mixed with Tween 20
TBST	tris-buffer-saline mixed with Tween 20
RT	room temperature
TE	Tris-EDTA
NP-40	Nonidet P-40
BCIP	5-bromo-4-chloro-3-indolyl-phosphate
NBT	nitro blue tetrazolium
IP	immunoprecipitation
Co-IP	co-immunoprecipitation
SDS-PAGE	sodium dodecyl sulfate-polyacrylamide gel
RT-PCR	reverse transcribed-polymerase chain reaction
dH_2O	distilled water
NF-κB	nuclear factor kappa-B
JAK-STAT	Janus kinase-Signal Transducer activator of transcription
ISGs	Interferon Stimulated Genes
TLRs	Toll-like receptors
PRR	pathogen recognition receptors
RLRs	RIG-I-like receptors
CLRs	C-type lectin receptors
NLRs	NOD-like receptors
RIG-I	retinoic acid inducible gene-I
MDA5	melanoma differentiated associated factor 5
LGP2	laboratory of genetics and physiology 2
RD	repressor domain
CTD	C-terminal domain
CARD	caspase recruitment domain
PAMPs	pathogen associated molecular patterns

MAVS	mitochondria anti-viral signaling protein
IPS-1	interferon-β promoter stimulator-1
Cardif	CARD adaptor inducing interferon-β
VISA	virus-induced signaling adaptor
MITA	mediated of interferon-β signaling adaptor
STING	stimulator of interferon genes
IKK	IκB, inhibitor of kappa-B
FADD	Fas-associated death domain
EGFP-	enhanced-green fluorescence protein
RFP-	red-fluorescence protein
FACS	fluorescence-activated cell sorting
IRFs	interferon regulatory factors
TRADD	TNF-receptor associated death domain
RIP1	receptor-interacting serine/threonine-protein kinase 1
TRAF3/6	Tumor necrosis factor (TNF)-associated factor 3/6
dsRNA	double-stranded ribonucleic-acids
SG	stress granule
mRNA	messenger ribonucleic acid
HuR	Hu protein R
PABP1	poly(A)-binding protein-1
TIA-1	T-cell intracellular antigen-1
TIAR	T-cell intracellular antigen-related proteins
G3BP1	Ras-GAP-SH3 binding protein-1
FRAP	fluorescence resonance after photobleaching
p54/Rck	ATP-dependent RNA helicase p54/B-cell lymphoma cell lines
PB	processing body
MEF	mouse embryonic fibroblast
OAS	oligoadenylate synthetase
DMEM	Dulbecco's Modified Eagle's medium
adeno-WT5	Adenovirus wild-type 5
adeno5ΔE1A	Adenovirus type 5 with deletion in E1A gene
DV	Dengue virus
EMCV	Encephalomyocarditis virus

HCV	Hepatitis C virus
HSV1	Herpes simplex virus-1
IAVΔNS1	Influenza virus non-structural protein-1 mutant virus
IAV WT	Influenza virus wild-type
NDV	Newcastle disease virus
PV	Poliovirus
SeV	Sendai virus
SINV	Sindbis virus
vSG	virus-induced stress granule
VSV	Vesicular stomatitis virus
VV	Vaccina virus
WNV	West Nile virus
PFA	paraformaldehyde
siRNA	small-interfering ribonucleic acids
qPCR	quantitative polymerase chain reaction
RNP	ribonucleoprotein
PKR	protein kinase R
eIF2α	eukaryotic initiation factor 2-alpha
GCN2	general control nonrepressed-2
HRI	heamoglobin regulated inhibitor
PERK	pancreatic endoplasmic reticulum eIF2-alpha kinase
GEF	guanosine exchange factor
Met	methionine
GTP	guanidine-triphosphate
TC	ternary complex
PIC	pre-initiation complex

CHAPTER 1

INTRODUCTION

1.1   Introduction

During the past decades, interferon (IFNs) system has been extensively characterized and proven for its indispensable role in mounting the first line defense against various types of infectious microbes. Basically we can classify this system into two categories—Type I and Type II IFNs system. The family members for Type I interferon include interferon alpha/beta superfamily, while the family member for Type II interferon include interferon-gamma. These proteins are specifically produced by cells after viral infection to inhibit their propagation. In viral infected cells, various signaling pathways are being activated, transmitting signals to downstream and further activates the specific families of transcription factors such as Interferon Regulatory Factors (IRF3, IRF7 etc), ATF2/c-jun, and Nuclear factor kappa-B (NF-κB) for the transcription of IFN genes. Secreted IFN-proteins outside the cells will bind to the cell surface interferon receptors. The binding with these receptors will further activate

another signaling pathway known as Janus kinase-Signal transducer activator of transcription, abbreviated as JAK-STATs. This signaling cascade further activates the expression of various interferon-stimulating genes (ISGs). These ISGs will in turn suppress viral replication through various modes such as RNA degradation and etc.

The underlying mechanism on how all these cytokines and ISGs are being produced, aspects ranging from signal transduction to the activation of transcription factors, which activates their expression within the nucleus, have always been the particular interests of many scientists working in this field. Scientists believe that sensors or detectors that could specifically differentiate between the distinct molecular structures broadly shared by pathogens and the host cells do exist (Janeway, C.A. 1989). During the past decades, extensively studies were performed to identify the presence of these receptors, which are termed as "pathogen recognition receptors" (PRRs). Up to recent date, major PRRs that have been successfully identified include Toll-like receptors (TLRs), NOD-like receptors (NLRs), RIG-I-like receptors (RLRs) and C-type lectin recrptors (CLRs) (Akira, S et al., 2006). CLRs were reported to sense the C-type lectin-like domain, which mainly found in fungus and bacteria, while various studies demonstrated that NLRs are mainly responsible for the intracellular inflammatory responses (Kawai, T & Akira, S. 2009). TLRs are well known for their detection of broad range of pathogens (Kawai, T. & Akira, S. 2010), including both bacterial and viruses. However, RIG-I-like receptors are still major sensors for viruses, which mainly deliver and replicate inside the cell cytoplasmic region.

In the next section of this chapter, I will briefly describe some of the underlying mechanisms of RIG-I-like receptors-mediated interferon systems in

response to viral infection. The significant roles of other PRRs such as NLRs, CLRs and TLRs have been reviewed elsewhere (Akira, S. et al. 2006) and will not be discussed in detail in this report.

1.2   RIG-I-like receptors and the signaling pathway

The family of RIG-I-like receptors plays an essential role as a sensor in detecting cytoplasmic viruses. RLRs recognize the distinct molecular structures which commonly found in viral RNA species. RLRs belong to the family of DExH/D box RNA helicase, which mainly comprises of three components—RIG-I (Retinoic acid inducible gene I); MDA-5 (Melanoma Differentiation Associated Protein 5) and LGP2 (Laboratory of genetics and physiology 2) (Yoneyama, M. et al. 2004). Schematic diagrams (Figure 1.0) indicated that all three RLR family members possess a DEAD box RNA helicase domain with ATPase activity. Both the RIG-I and LGP2 share the homology of the domain called repressor domain (RD). This domain located within the C-terminal region of both components as compared to MDA5. It was demonstrated that the repressor domain mainly functions as an "autoregulator", involve in regulating the functions of both RIG-I and LGP2 during quiescent and active state. At the N-terminal side, both RIG-I and MDA-5 shared a similar region known as Caspase-Recruitment Domain (CARD). However, this domain is not identified in another family member LGP2 (Figure 1.0). Various reports have further characterized the specificities of each RLR members for various viruses. For example, RIG-I specifically recognizes viruses from the family of Orthomyxoviridae, Paramyxoviridae and Rhabdoviridae, whereas MDA5 specifically recognizes positive

3

strand viruses, mainly from the family of Picornaviridae (Kato, H. et al. 2005; Yoneyama, M. et al. 2005; Kato, H. et al. 2006).

Beside their specificity, the underlying mechanisms on how RLR members transmit signals were also extensively studied. Under the quiescent state, both RIG-I and MDA5 remains in a closed conformation. After viral infection, the repressor domain located within the C-terminal domain of these two components could detect the presence of triphosphate moieties at the 5'-terminal of viral genomic RNA. These tri-phosphate moieties cannot be found in the host mRNA species as they are masked by the presence of 5'-capped structure. Hence, RLR members such as RIG-I will recognize this structure as the PAMPs, which in turns activates RIG-I, inducing the conformational change to an "open" form by releasing the CARD domain (Takahasi, K. *et al.,* 2008; Yoneyama, M. & Fujita, T., 2010). The "active open form" of RIG-I will form a homotypic CARD-CARD interaction with its downstream signaling adaptor called MAVS (also known as IPS-1, CARDIF or VISA) (Kawai, T. et al. 2005; Meylan, E. et al. 2005; Seth, R.B. et al. 2005; Xu, L.G. et al. 2005). This interaction further induced the recruitment of numerous signalling components such as TNF receptor-associated death domain (TRADD) (Michallet, M.C. et al. 2008), Fas-associated death domain (FADD) (Balachandran, S. et al. 2004), TRAF3 and 6, RIP1 (Saha, S.K. et al. 2006; Yoshida, R. et al. 2008), stimulator of interferon genes (STING, also known as MITA, ERIS or MYPS) (Ishikawa, H. & Barber, G.N., 2008; Jin, L. et al. 2008; Zeng, W. & Chen, Z., 2008; Zhong, B. et al. 2008; Sun, W. et al. 2009) and etc. All these components will form a large signaling complex termed "signalosome", which in turn relays the signals to downstream and further activates

the IKK canonical complexes, followed by activation of transcription factors such as IRF3 and NF-κB to induce the expression if Type I interferon genes (Figure 2.0).

1.3   Interferon inducible proteins

RLR-mediated production of type I interferon in response to viral infection will triggered the substantial production of numerous cellular proteins (Der, S.D. et al. 1998). Since the expression of these proteins can only be triggered by interferon, they were all classified as "interferon-inducible proteins". Numerous studies have indicated that these components also play an essential role in host defensive system, contributing to suppressing viral infection by targeting at multiple levels. Some of these proteins possess functions similar to RLR members, which could recognize PAMPs of viruses such as triphosphate or double-stranded RNA structures (dsRNA). One of the examples would be a protein known as serine-threonine protein kinase-R (PKR) (Clemen, M.J. & Elia, A., 1997). During the quiescent state, cells maintain a low expression of PKR. However, the expression was enhanced after viral infection. PKR proteins contain a dsRNA-binding domain, after engagement with the ligand dsRNA, PKR will be activated through autophosphorylation to exert its antiviral functions (Nallagatla, S.R. et al. 2007).

In addition to its antiviral responses, activated form of PKR also known to involve in many important cellular functions. Cell initiate series of rapid reprogramming in response to various environmental treatments, activating the cellular stress response pathway, which is another well-known pathway that involved PKR. In this pathway, activated form of PKR will then phosphorylate its downstream

5

adaptor, eukaryotic translation initiation factor 2-alpha (eIF-2α) for transmitting signaling. It would be an interesting topic for us to explore the underlying significance of this PKR-mediated cellular stress pathway from the perspective of host defense.

1.4   Stress response pathway and stress granule components

There are high possibility that cells might be exposed to various environmental cues such as deprivation of glucose, heat shock or a drastic change in temperature, UV radiation, chemical treatment and etc. These types of circumstances might possess a danger threat towards the cells. Under such circumstances, cells initiate series of reprogramming on their cellular events to protect the host—one of the key pathways is the cellular translation machinery. When cells are exposed to such threats, activated form of cellular kinases such as Protein Kinase R (PKR), General Control Nonrepressed-2 (GCN2), Haemoglobin Regulated Inhibitor (HRI) or Pancreatic Endoplasmic Reticulum eIF2-alpha kinase (PERK) will phosphorylate their downstream component called eukaryotic initiation factor 2-alpha (eIF2α). The activation of eIF2α will further enhances its binding affinity with its substrate termed Guanosine Exchange Factor (GEF), and thus, inhibiting the formation reused of eIF2α-GTP-Met-tRNAi ternary complexes (TC) by inhibiting the recycling of eIF2α-GTP complexes back to the on going translation machinery. These phenomena further disperse the stable form of polysomes and hence, result in the accumulation of pre-formed 48S pre-initiation complexes (PIC), followed by the inhibition of cellular protein synthesis. Under such circumstances, the translation process of host messenger RNA will be terminated, and arrested mRNA transcript will be re-assorted and

compartmentalized in a dense, non-membranous cellular entity called stress granules (SG) (Anderson, P. & Kedersha, N. 2002; Thomas, M.G. et al. 2011).

The major purpose for cells to initiate such type of reprogramming is to prepare the host to adapt to the sudden change of the extracellular environment. The stalling of PIC could provides additional time for cells to repair the damages, which could eventually lead apoptosis or cell death. Therefore, the transient re-assortment of cellular host mRNA inside the stress granule could further protect these naked mRNA transcripts from being damaged by the stress. The composition of stress granules mainly comprises of the 48S PICs, together with numerous RNA binding proteins such as PABP1, a poly(A)-tail binding protein, HuR, an AU-rich binding protein, T-cell Intracellular antigen-1 (TIA-1/R), Ras-GAP-SH3 binding protein-1 (G3BP1) and etc.w (Thomas, M.G. et al. 2011). FRAP analysis further demonstrated that components within the stress granules constantly, and rapidly shuttle in and out, either back to the cytoplasm, or shuttle to another cytosolic compartment called Processing Body (abbreviated as "P-body" or "PB"). P-body is a tiny cytoplasmic foci that is well-known for an essential role in mRNA decay. These foci are found to evenly distribute throughout the cytoplasm under quiescent state. Under stress response, P-body foci are recruited and juxtaposition with stress granule (Kedersha, N. et al. 2000; Hoyle, N.P. et al. 2007). Since all the aforementioned proteins possess essential roles in RNA metabolism, these further highlight the importance of stress granule to serve as a multipurpose platform for sorting, remodelling and re-assortment of host mRNA for re-initiation of translation, storage, or to PB for degradation.

Among the aforementioned proteins, studies revealed that at least two RNA binding proteins—both TIA-1/R and G3BP1, play a critical role in stress granule formation and assembly. These two components act downstream of eIF2α. Study indicated that overexpression of G3BP1 will further induce the oligomerization and hence the formation and assembly of stress granule. Activation of G3BP1 also requires its phosphorylation. Mutagenesis analysis at the phosphorylation site, amino acids position 149 of G3BP1 significantly impaired the formation of stress granule (Tourrière, H. et al. 2003). As for TIA-1, stress granule formation was completely inhibited in TIA-1 deficient MEF cells after arsenite treatment (Gilks, N. et al. 2004). However, TIA-1 might not be an essential component for SG formation in response to heat shock (Lopez de Silanes, I. et al. 2005; Grousl, T. et al. 2009). These support the notion that the nature of stress could be the key to determine the formation and the assembly rules of SG.

1.5   Virus-induced stress granule and roles in antiviral

Viral infection is also a phenomenon that could signal the "threat alarm" for host cells. Beside interferon and ISGs, cellular stress response pathway is also initiated after viral infection. PKR, an interferon-inducible protein, will be activated after detecting it's ligand, dsRNA. As described in Section 1.3, this activated form of PKR will phosphorylate its downstream substrate, eIF2α and induces the formation of SG. Since the nature of stress is viruses, in this context onwards, the term "virus-induced stress granule" (vSG) will be used to describe these phenomena.

From the discussion in Section 1.3, the formation cytoplasmic SG, which mainly comprise of stalled 48S PICs, could also stalled viral RNAs, preventing the continuous translation of viral mRNAs to viral proteins. These eventually suppress viral replication through the inhibition of viral protein synthesis. These further shed some light on the importance roles of vSG in antiviral. Moreover, we previously identified that numerous critical antiviral components such as RLRs, OAS, RNase L are being recruited into vSG (Onomoto, K. et al. 2012), further strengthening the notion that vSG serve as a vital cellular entity for antiviral. The recruitment of RLRs to vSG poses a hypothesis in which these compartments might involve in regulating cellular IFN response, either through a direct or indirect manner. Therefore, it is tempting to initiate an investigation line to understand the functional roles of vSG from the perspective of host innate immune response.

In addition to that, many recent studies revealed that there was active bidirectional interaction between viruses and SG. Different types of viruses possess different modes or strategies to modulate stress granules formation. Apart from them, many reports have concomitantly demonstrated that viruses have evolved various strategies to inhibit stress granule formation and/or their assembly (Iseni, F. et al. 2002; Li, W. et al. 2002; Emara, M.M. & Brinton, M.A. 2007; White, J.P. et al. 2007), proposing a notion that vSG formation could interfere the viral replication inside the host cells. In this dissertation, there are several objectives. The first aim is to understand the mode of cytoplasmic SG formation after infected with both RNA and DNA viruses through the development of cell-based fluorescent reporter system, and monitoring through live-cell imaging. The second objective would be delineating the

underlying modes of SG modulation by focusing on one virus. Then I will focus on understanding whether vSG is critical for host innate immune response and how.

1.6   Primary Research Objectives

The main objectives of this thesis are:

(i)   To examine the general physiological impact on SG formation and its modulation by both RNA and DNA viruses.

(ii)   To further understand the underlying modes of SG modulation of one specific virus.

(iii)   To examine the functional role of vSG from the perspective of viral replication and host innate immune responses.

(iv)   To delineate the underlying mechanism(s) involved in point (ii).

CHAPTER 2

RESULTS

2.1 Characterization of HeLa cells stably expressing SG marker, G3BP1.

2.1.1 Homogeneity of G3BP1 expression in all stable clones

This project begins with the aim of understanding the mode of SG modulation by various types of viruses. To investigate this, I established a cell-based fluorescent system by using G3BP1, a well-known stress granule marker as the representative of SG formation. However, this experimental system involved the transient overexpression of chimerical SG probe tagged with fluorescent protein. Previous studies indicated that such system might interfere with the normal cellular stoichiometry, resulted in the formation of aberrant structure. Moreover, constitutive aggregation of intrinsic SG components could lead to severe halt in protein synthesis, resulting in various side effects such as slow cell growth rate, or

more severe, cell death or apoptosis (Kedersha, N. et al. 2008; Kharraz, Y. et al. 2010). Hence, I performed additional experiments to verify the system I established. Firstly, to confirm whether the SG-fluorescent labelled chimerical cells are displaying normal cellular stoichiometry, several quality control and functional assays were performed. I screened out the clones which stably expressing EGFP-G3BP1 and G3BP1-pDsRed by using antibiotics and verified their expression through confocal microscope. I also examined the expression level of these fluorescent proteins by using flow cytometry and sorted out the single cells with equal expression level. Results from these two approaches indicate that all the selected HeLa stable clones showed homogeneity and high expression level at each single cell unit respectively. Most importantly, SG formation is not observed under the quiescent state (**Figure 3A**), suggesting that intrinsic stress response pathway within all stable clones was not initiated due to artefacts results from overexpression system. For the convenience of my subsequent experiment, I have decided to use only the stable clones expressing EGFP-G3BP1.

2.1.2 HeLa EGFP-G3BP1 stable cells responded normally to oxidative stress

Next, I examined whether all these selected stable clones can behave normally in terms of functions. It is well known that arsenite treatment, which is a type of oxidative stress, could induced the significant aggregation of G3BP1 to form cytoplasmic stress granules. Therefore, this system should also exhibit the similar phenotype if they behaved normally. To verify this, immunostaining analysis was

performed with all HeLa stable clones treated with arsenite for 1 hour, and GFP localization was examined under microscope. Results indicate that all these stable clones displayed G3BP1 granules formation after arsenite treatment. Data from HeLa clone#12 was chosen as a representative image (**Figure 3B**). The percentage of cells for all clones forming G3BP1 granules was quantified and presented in a bar graph as shown in **Figure 3C** (*upper*). These results indicate that all stable clones responded normally to oxidative stress.

2.1.3 HeLa EGFP-G3BP1 stable clones responded normally to viral infection.

As demonstrated by our laboratory (Onomoto, K. et al. 2012), viral infection also induces the formation of SG. To verify that these stable clones could function normally in response to viral infection, all EGFP-G3BP1 stable clones were "Mock" treated or infected with IAVNS1 or NDV for 9 hours. Cells were fixed and analysed for G3BP1 granule formation under microscope. Results indicate that all selected HeLa EGFP-G3BP1 stable clones displayed significant formation of G3BP1 foci. A representative images from stable clone#12 was depicted in **Figure 3B**. Similarly, the efficiency of these stable clones in forming foci was examined. Percentage of cells forming G3BP1 foci within all clones was quantified. Results indicate that an average of approximately 65.7% of cells displayed G3BP1 foci formation in each clone [**Figure 3C** (*lower*)]. These results demonstrate that all selected HeLa EGFP-G3BP1 stable clones responded efficiently to viral infection.

2.1.4 IFN-β signalling is normal in all HeLa EGFP-G3BP1 stable clones.

Since I have interest to use these cells for the study of innate immunity, I further confirmed that the host innate immune response in these stable cells was not affected. To verify this, all HeLa EGFP-G3BP1 stable clones were "mock" treated or infected with NDV for 12 hours, and determined the induction of IFN-β mRNA through RT-qPCR. Results indicated that comparable amount of IFN-β mRNA induction was observed in all stable clones (**Figure 3D**) when compared to parental cells. Hence, these results imply that the interferon signalling in all these stable clones are responded normally after viral infection.

In addition, no retardation in cell growth and no significant of cell death was observed among all these stable clones. Collectively, all the selected HeLa EGFP-G3BP1 stable clones could behave normally and I have chosen clone#18 for my subsequent experiments.

2.2 Both RNA and DNA viral infection induces G3BP1 to displayed three subcellular redistribution patterns

As described in the Chapter 1, Section 1.6, we are interested in the modulation of SGs by various types of viruses. Soon after the establishment of HeLa EGFP-G3BP1 stable cells, I further examined the dynamism of SGs after infection with both RNA and DNA viruses. Real-time monitoring provided us the advantage of visualizing the modulation of SG in time-lapse, covering the entire framework—start from viral entry up to the edge of progressive replication. Imaging was immediately initiated after 1 hour post infection, with images captured every 10 mins. Result indicated that HeLa EGFP-G3BP1 WT stable cells started to display G3BP1 redistribution at an average time range of 5-6 hours post-infection. Small granules start to form, and gradually being assemble and fused to a bigger granule. Results also indicated that positive strand viruses of Picornavirus family such as PolioV and EMCV tend to form SGs at a much earlier time point ($\approx$ 4 hours) when compared to other RNA and DNA viruses. Strikingly, different viruses tend to induce different modes of G3BP1 redistrubution patterns. Results from quantification of cells with SG formation demonstrated that I could classified the aggregation patterns into three distinct forms, namely—stable formation, transient formation and alternate formation (**Figure 4A**). Cells infected with NDV (**Figure 4B**), IAVΔNS1 (**Figure 4D**), and Adenovirus type 5 (**Figure 4K**) showed stable SG formation; while EMCV (**Figure 4E**), SINV (**Figure 4F**), and PolioV (**Figure 4G**) infected cells showed transient SG formation. Only Adeno5ΔE1A infected cells displayed alternate SG formation (**Figure 4J**). I observed no SG formation in

cells infected with IAV (**Figure 4C**), VSV (**Figure 4I**), TMEV (**Figure 4L**), and SeV (**Figure 4H**).

Taken together, these results indicate that cellular stress response is initiated after viral infection. Real-time monitoring further shed some lights on our understanding towards the dynamic nature of SG induced by both RNA and DNA viruses, providing instrumental information for further characterization in the future. In addition to that, different viruses induce different subcellular redistribution pattern of SGs, suggesting that different viruses are modulating SGs through different modes. I further focus on EMCV in my subsequent analyses.

2.3   EMCV infection results in the cleavage of G3BP1 through its 3C protease.

2.3.1   The transient formation is due to the cleavage of G3BP1

Results from real-time imaging demonstrated that EMCV induces transient formation of SG. I asked what would be the underlying mechanism(s) that account for this phenomenon. Previous report indicated that SG was induced but dispersed at the later stage after PolioV infection, which is mainly due to the cleavage of G3BP1 by its 3C protease (White, J.P. et al. 2007). In my study of real-time monitoring using PolioV also displayed similar phenotype (**Figure 4G**), moreover, both EMCV and PolioV belong to the same family of *Picornaviridae*. This prompted me to ask whether the dispersion of SG by EMCV is also due to cleavage of G3BP1 by its viral protease. To verify this, I checked the protein

expression of G3BP1 at different time-point through western blot. Results indicated that G3BP1 was indeed, cleaved after EMCV infection [**Figure 5A** (*upper*)]. The cleavage produces detectable level of a huge protein fragment containing GFP-tagged with molecular weight of approximately 80-kDa after 6 hours post-infection, with the complete cleavage of EGFP-G3BP1 occurred after 10 hours post-infection.

2.3.2   Cleavage occurred at C-terminal region of G3BP1

Since the HeLa stable cells are expressing G3BP1 with GFP-tagged at the N-terminal region, the production of the huge fragment 80-kDa with anti-GFP antibody suggested that the cleavage site is likely to occur at the C-terminal region. To test this hypothesis, I utilized an antibody specifically targeting the C-terminal region of G3BP1. Western blot analysis with this antibody produces a smaller fragment of approximately 20-kDa (**Figure 6A**), which was not found in blotting with antibody targeting N-terminal region. This data implied that the cleavage of G3BP1 mainly occurred at the C-terminal region (**Figure 6B**). Since the cleavage phenomenon is similar to that of PolioV, I next examined whether the cleavage site of EMCV is similar to that of PolioV. To test this, I established another cell line which stably expressing FLAG-G3BP1 with single point mutation at amino acids position 325, which resist to cleavage by PolioV 3C. As depicted in **Figure 5A** (lower), no cleavage fragment of FLAG-G3BP1 was observed throughout the western blot analysis at different time points. This result

demonstrates G3BP1 is cleaved, with position (Q325) similar to PolioV after EMCV infection.

2.3.3   EMCV 3C protease cleaves G3BP1, dispersing SG formation.

Based on these similarities, the cleavage of G3BP1 by EMCV infection could be also due to its 3C protease. To conclusively verify this, I transiently overexpressed vector encoding EMCV 3C protease into HeLa parental cells. Results indicated that G3BP1 was indeed, cleaved by EMCV 3C protease [**Figure 5B** (*left*), lane 3]. Similar cleavage fragment was also observed in EGFP-G3BP1 WT cells but not in Q325E mutant cells after expressing EMCV 3C protease construct [**Figure 5B** (*right*), lane 3 and 6]. Hence, these data conclusively demonstrate that the cleavage is indeed, mediates through EMCV 3C protease.

After confirming the cleavage site and the protease involved, I re-examined the SG formation by using HeLa stably expressing EGFP-G3BP1 Q325E mutant through real-time monitoring. Comparing to WT, results indicated that Q325E mutant cells mainly displayed stable formation SG (**Figure 7A-B**). The percentage of cells showing stable SG formation pattern was quantified and presented in a bar graph as shown in **Figure 7C**. Taken together, all these results demonstrate that the transient formation of SG after EMCV infection is mainly due to the cleavage of G3BP1 mediated by its viral 3C protease.

2.4   No other SG components are cleaved after EMCV infection

As described in previous section, SG entity comprise of other cellular components. Dispersion of SG after EMCV infection might due to the cleavage of other components. To verify this, I examined the expression level of other SG components, which include PABP, TIA-1/R, HuR and PKR. Results indicated that neither of these components was cleaved after EMCV infection (**Figure 8A**). These data indicated that the dispersion of SG as observed after EMCV infection is solely due to the cleavage of G3BP1.

2.5   G3BP1 is critical to suppress EMCV replication.

Viruses tend to evolve strategies to evade host immune defence to facilitate their replication. Cleavage of G3BP1 by EMCV 3C protease could be also a type of such strategy. To examine the effect of G3BP1 cleavage on EMCV replication, I used two approached: (i) by measuring the EMCV RNA within the cell cytoplasm using RT-qPCR; (ii) by measuring the EMCV virions in the cell supernatant through plaque assay. Results indicated G3BP1 Q325E mutant stable cells can significantly suppressed the EMCV replication as compared to WT stable cells (**Figure 9A-B**). To further confirm this observation, siRNA targeting human G3BP1 was transfected to HeLa parental cells. Endogenous depletion of G3BP1 significantly potentiates EMCV replication (**Figure 9C-D**). Taken together, these results demonstrate that the core SG component, G3BP1 plays a critical role in suppressing EMCV replication.

2.6 G3BP1 plays an essential role in EMCV-induced interferon production.

2.6.1 G3BP1 is dispensable for early phase of IFN-induction.

After confirming that G3BP1 contributes to antiviral, I next asked what would be the underlying mechanism(s). Interferon systems play a critical role in protection against infectious microbes. I asked whether G3BP1 contributes to antiviral through IFN system. Since EMCV-induced SG was observed after 4-5 hours post infection, I examined the IFN-β mRNA induction at early time points, comparing both G3BP1 WT and Q325E mutant cells. Results indicated that no significant difference was observed in the kinetics of IFN-β mRNA expression in both WT and Q325E mutant cells (**Figure 10A**). I further test the expression of other cytokines and chemokine genes. The kinetics for CXCL10, IL-6 and RANTES mRNA expression was not affected as well (**Figure 10B-D**). This data implies that G3BP1 is not essential for the early phase of IFN-β gene induction.

2.6.2 G3BP1 is critical for the later-phase of IFN-induction.

I previously demonstrated that EMCV displayed transient SG formation. SGs are induced at the early time points, but dispersed at the later stage. Therefore, I asked whether G3BP1 regulates IFN-system at the later time phase of infection. By comparing both WT and Q325E mutant cells, I observed a significant inhibition of IFN-β mRNA levels in G3BP1 WT when compared with Q325E mutant cells after 8 hours post infection. The down regulation of IFN-β gene continues up to

16 hours post infection (**Figure 11A**). In addition, I performed ELISA assay to quantify the production of human IFN-β protein. Result indicated that an enhancement of IFN-β protein production within the culture supernatant after 24 hours post infection (**Figure 11B**). Similar results were obtained when I examined the induction level of CXCL10, IL-6 and RANTES mRNA in both WT and Q325E mutant cells (**Figure 11C-E**). Functional analyses by using siRNA targeting human G3BP1 consistently confirm this observation (**Figure 12A-D**). Collectively, these results imply that G3BP1 plays a critical role in regulating IFN-β gene induction at the later phase of EMCV infection. In agreement with these results, persistent IFN-β gene induction as observed in Q325E mutant cells also suggested that the down regulation at the later stage is due to cleavage of G3BP1 by protease, an evasion strategy by EMCV to survive in cells.

2.7   SG-dependent IFN system was impaired by EMCV 3C, not leader

It has been suggested that leader protein of Picornaviruses is the key factor to suppress IFN-β production (Pesch, V.V et al. 2001). Moreover, in some recent reports using TMEV, a virus belongs to the same genus of "Cardiovirus" as EMCV, demonstrated that TMEV leader protein is essential in inhibiting both SG formation and TMEV-induced IFN-β production (Borghese, F. & Michiels, T. 2011; Langereis, M.A. et al. 2013). To clarify the role of EMCV 3C and leader, I transiently overexpressed vectors encoding each protein respectively, and monitor both SG formation and IFN-β production. Results indicated that overexpressed of

EMCV 3C inhibit arsenite-induced SG formation but not leader (**Figure 13A**). Moreover, no cleavage fragment was observed in western blot analysis [**Figure 5B** (*right*), lane 2 and 5]. Simultaneously, I observed a significant inhibition of polyI:C-induced IFN-β gene after overexpressing both leader and 3C (**Figure 13B**). These data indicated that in the case of EMCV, both leader and 3C impaired IFN-β gene activation, but SG formation was not affected by leader, suggesting inhibition by 3C mainly affects SG dependent-IFN-β, while inhibition by leader could be through a different pathway.

2.8   Sensor for EMCV, MDA5 is recruited to SG.

2.8.1   MDA5 is recruited to SG after EMCV infection.

Since dispersion of SG impaired EMCV-induced IFN production (Section 2.5). I next asked what are the underlying mechanism(s). As reported previously, RIG-I is recruited into SG after IAVΔNS1 infection (Onomoto, K. et al. 2012). Since EMCV is preferentially recognized by the RLR sensor, MDA5 (Kato, H. et al. 2005; Kato, H. et al. 2006), I asked whether SG regulates IFN through MDA5. To test this, I performed immunostaining analysis and observed the subcellular distribution of MDA5 with specific antibody. In order to prevent the dispersion of SG, I fixed cells at early time point after infection. Results indicated that MDA5 is recruited into SG marker such as G3BP1 and TIAR after EMCV infection (**Figure 14A-B**). Co-staining with propidium iodide (PI) further indicated that EMCV dsRNA, which is the ligand for MDA5 activation, are also co-localized

with both MDA5 and SG components (**Figure 14A-B**). These results demonstrate that SG modulates IFN system through the recruitment of MDA5 and EMCV dsRNA.

2.8.2   RIG-I expression was not affected in PolioV and EMCV infection.

Previous studies indicated that both RIG-I was degraded in both EMCV and PolioV infection and hence, down-regulation of IFN system was observed (Barral, P.M. et al. 2009). To clarify this, I performed western blotting to examine the protein expression of RIG-I. Results indicated RIG-I was not cleaved after EMCV (**Figure 15A**) and PolioV (**Figure 15B**) infection. These data indicates that the dysfunction of IFN-system as observed after EMCV infection is not due to the cleavage of RIG-I as reported previously, but due to the dispersion of SG by EMCV protease.

2.9   PKR plays a vital role in both EMCV-induced SG and IFN-β induction.

2.9.1   PKR is critical for EMCV-induced SG formation.

As described in Chapter 1, Section 1.3, PKR is one of the essential components for mediating cellular stress response. Numerous studies have indicated that the many viruses induce SG formation by activating dsRNA kinase PKR. To verify whether PKR is also essential for EMCV-induced SG formation. I used siRNA approach. Two different siRNAs targeting human PKR were transfected into

HeLa parental cells and infected with EMCV. Immunostaining was performed to monitor endogenous SG formation. Data indicated that EMCV-induced SG formation was significantly impaired after depleting PKR (**Figure 16A**). Quantification of cells forming SG comparing both control and PKR siRNA transfected cells after EMCV infection was presented in the bar graph (**Figure 16B**). Since EMCV infection resulted in G3BP1 cleavage, I asked whether cleavage of G3BP1 might affect PKR activation. Data from western blot indicated that PKR was phosphorylated after 4 hours post-infection, but was dephosphorylated at 12 hours post infection (**Figure 16C**, lane 2 and 3). The dephosphorylation of PKR is corresponded to the cleavage of G3BP1 (**Figure 16C**, lane 3). The replication level of EMCV was confirmed by specific antibody targeting EMCV 1AB and 1D proteins (**Figure 16C**, lane3). These data indicate the cleavage of G3BP1 by EMCV 3C protease resulted in the dephosphorylation of PKR, and hence, dispersing SG formation.

2.9.2   PKR is essential for EMCV-induced IFN-β gene activation

Finally, I examined the effect of PKR on IFN-β gene activation. To test this, I quantified the IFN-β mRNA expression levels in PKR depleted HeLa parental cells by using RT-qPCR. Results indicated that IFN-β gene induction was significantly impaired in PKR depleted cells after EMCV infection (**Figure 16D**). The impairment of IFN-β signalling after polyI:C and IAVΔNS1 infection were consistent as we previously observed (Onomoto, K. et al. 2012) and were used as

a control in this study. Taken together, these results indicate that PKR plays an indispensable role in both EMCV-induced SG formation and IFN-β gene activation.

CHAPTER 3

DISCUSSION

The production of type I interferon has always been the major weapon to combat viral infection. The engagement of extracellular interferon proteins with transmembrane interferon receptors further induces the expression of approximately three hundreds ISGs in neighbouring cells, strengthening the host defensive lines. In addition to its well-known antiviral functions, one of the ISGs, PKR, also play an essential role in host cellular stress pathway. PKR will be activated after detecting dsRNA and induces the formation of a dense and non-membranous cytoplasmic foci known as stress granules. Summarized from most of the current findings, formation of vSG has been ascribed for both positively and negatively regulating viral replication (Emara, M.M. & Brinton, M. 2007; White, J.P. et al. 2007; Qin, Q. et al. 2009; Simpson-Holley, M. et al. 2011). However, detailed mechanistic actions are still not being sufficiently elucidated. These prompted us to initiate the investigation line to further delineate the underlying functional roles of vSG.

In this study, I describe about the critical role of virus-induced SG in regulating virus-induced IFN responses and how viruses evolve strategies to counteract this defensive line. Since the formation and assembly process of SG formation could plays an essential role in host antiviral response, it is important to understand how different viruses modulate this process. From this study, I discovered that viral infection induces three distinct types of SG redistribution patterns, namely stable formation, transient formation and alternate formation. Viruses such as SeV, IAV and TMEV do not induce SG. It is suggested that SeV RNA trailer, NS1 protein of IAV, and the leader protein of TMEV are those which responsible in inhibiting SG formation (Iseni F. et al. 2002; Borghese F. & Michiels T. 2011; Onomoto, K. et al. 2012). These observations are consistent with the quantification data of my real-time analyses (Figure 4B). A recent report utilizing elegant computational study to demonstrate that the pattern of alternate formation, in which SG appear, disappeared and re-formed, is mainly regulated through the dynamic equilibrium between the host cellular response and viral pathogenesis (Ruggieri, A. et al. 2012). However, detail mechanistic actions are still remains in cold midst, further clarification is required.

Previous study has shown that poliovirus, which belongs to the family of *Picornaviruses,* inhibits the formation of cytoplasmic SG in the later stage by cleaving G3BP1 through 3C protease (White, J.P. et al. 2007). In this study, I observed the similar result of transient SG formation through real-time monitoring of PolioV and EMCV infection. Based on this information, I speculate that EMCV might display the similar strategy as PolioV in inhibiting SG formation. Indeed, by using the stable cells system, I can observe the presence

of G3BP1 cleavage fragment. This cleavage fragment was detected at the lower level at the early time point of infection ($\approx$ 4 hours), and gradually appeared as infection prolongs. The complete cleavage fragment is observed at the later stage of post-infection ($\approx$ 10 hours). This data is consistent with my observation in imaging analyses, in which SG is induced at the beginning time point and dispersed at the later phase after EMCV infection. By using the Q325E stable mutant cells and overexpressing the plasmid encoding EMCV 3C system, I confirmed that G3BP1 is cleaved by EMCV 3C protease at position of Q325, which is locating at the C-terminal region. On going viral replication is necessary for the accumulation of viral protease, which accounts for the cleavage at the later phase.

It is suggested that another *Picornaviruses*, TMEV, which belongs to the sub-genera of *Cardioviruses,* inhibit SG formation through leader protein (Borghese, F. & Michiels, T. 2011). Since EMCV also belongs to the same sub-genera as TMEV, I tested EMCV leader protein through overexpressing system. Surprisingly, arsenite-induced SG formation was not impaired, indicated that the dispersion of SG formation is solely due to the cleavage by EMCV 3C protease. Interestingly, in another recent study using coxsackievirus (CVB3) also demonstrated that SG formation was inhibited through a similar mechanism (Fung G. et al. 2013), suggesting that the similar strategy is used by some positive strand viruses to evade cellular stress response.

Pro-viral and anti-viral characteristics are often being ascribed to the functions of vSG. In this study, I observed that EMCV replication is efficiently suppressed in Q325E mutant

stable cells. This data is also consistent with siRNA depletion analyses, indicating that SG is critical to block EMCV replication. In the similar Q325E mutant stable cells system, I also observed the enhancement of IFN-β production at the later stage after EMCV infection. Endogenous depletion further confirmed this observation. This data suggest that the observed enhanced of EMCV replication is mainly due to the blockage of IFN-β signalling. This also indicated that G3BP1 is essential for EMCV-induced IFN-β, exhibiting the similar functions as observed in IAVΔNS1 infection (Onomoto, K. et al. 2012). It is suggested that the EMCV degrades RIG-I, and subsequently impaired the IFN-β production (Barral, P.M. et al. 2009). However, I do not observe these cleavages in my study (Figure 15), excluding the possibility that the impairment of EMCV-induced IFN-β signalling is due to the degradation of RIG-I. In non-infected state, the RIG-I antibody used by Barral et al. detects un-cleaved RIG-I at the molecular weight of approximately 60 kDa, however, it is well characterized that the actual molecular size of RIG-I is approximately 117 kDa (Takahasi, K. et al. 2008). Therefore, whether the RIG-I antibody used by Barral et al truly detects the genuine RIG-I protein still remained to be clarified. Moreover, previous analysis with RIG-I deficient fibroblast cells still showed robust IFN-β production in response to EMCV infection (Kato, H. et al. 2006), indicating that RIG-I is dispensable for EMCV-induced IFN-β signalling.

What would be the underlying mechanism on how SG modulating EMCV-induced IFN-β signalling? I found that SG modulates EMCV-induced IFN-β signalling by recruiting it's specific sensor MDA5 to SG. Moreover, as observed with the presence of dsRNA stained by propidium iodide, subcellular re-distribution of MDA5 to SG increases the local

concentrations of this sensor within the condensed foci, which is likely that account for a more efficient PAMPs detection, and hence, facilitates a more persistent activation of IFN-β signalling at the later time point. However, it is suggested that EMCV produces high-molecular RNA web, which is responsible for MDA5 activation (Pichlmair, A. et al. 2009). Therefore, it remains to be determined whether this RNA web can be found in SG. Furthermore, I also clarified that EMCV-induced SG is absolutely dependent on PKR, as deletion of PKR significantly abrogates EMCV-induced SG formation and IFN-β production. Although EMCV leader does not affect SG formation, but it's overexpression still suppressed IFN-β, suggesting that leader protein of cardioviruses could function similarly, or the inhibition occurred through non-SG dependent pathway. Taken together, all the data above suggest that EMCV infection induces SG formation at the early stage, SG assembly further recruits the RNA sensor MDA5 and concentrated this protein within a condensed foci, enhances the detection of dsRNA, which facilitates higher production of IFN-β production. However, prolong EMCV replication accumulates sufficient amount of viral protease 3C, which cleaves G3BP1, dispersed SG and hence, inhibiting the IFN-β production. Highlighting the significant role of SG in innate immune response.

CHAPTER 4

EXPERIMENTAL RATIONALE

4.1   Viruses and plasmids constructs

Viruses used in this study includes Vesicular stomatitis virus (VSV; Indiana
strain), Encephalomyocarditis virus (EMCV), Sindbis virus (SINV), Theiler's
Murine encephalomyelitis virus (TMEV; GDVII strain), Poliovirus (PV;
Mahoney strain), Adenovirusese (Strain type 5), Newcastle disease virus (NDV;
Miyadera strain), Sendai virus (SeV; Cantell strain), and Influenza A virus with
deletion of the NS1 gene (IAVΔNS1; strain A/Puerto Rico 8/34). VSV, PV,
EMCV, adenoviruses and TMEV were propagated by using an IFN non-
producing cells, BHK21. After infection at a multiplicity of infection (MOI) of 1,
BHK21 cells were incubated at 37°C for several days until all cells were
confirmed die. Cell culture medium containing newly propagated viruses were
collected and subjected to centrifugation at the speed of 1,500 rpm for 5 min to
precipitates the death cell debris. The supernatant was recovered and subjected to

plaque assay to determine the viral titer. Viruses like NDV, SeV and IAVΔNS1 were propagated in the allantoic cavities of embryonated chicken eggs. All viruses stock were store at -80°C, and the infection work were performed in the UV-sterile bench with Biosafety Level 2, following protocols and guidelines as designated by Kyoto University.

Expression vector encoding stress granule marker, EGFP-tagged Ras-Gap SH3 domain-binding protein 1 (pEGFP-G3BP1; NCBI RefSeq accession no: NM_005754) was kindly provided by Dr. Jamal Tazi (Institute de Génétique Moléculaire de Montpellier, France) (Tourrière H et al. 2003). Plasmid constructs encoding EMCV Leader protein (pF-Leader) and 3C proteases (pF-3C) were kindly provided by Dr. A.C Palmenberg (Institute for Molecular Virology, University of Wisconsin-Madison). The mutant expression vector pEGFP-G3BP1 Q325E (amino acid changed from glutamine to glutamate) was generated by site-directed mutagenesis, under the standard protocols as recommended by the KOD-Plus mutagenesis kit (Toyobo, Japan). The construct was then sequenced to verify the presence of the mutation.

4.2   Generation of HeLa cells stably expressing fluorescent-tagged SG marker
HeLa cells stably expressing stress granule marker, expression vectors pEGFP-G3BP1 wild-type (WT) and pEGFP-G3BP1 Q325E mutant were linearizing by using the restriction enzyme ApaL1 (Takara, Japan). The linearization was confirmed on agarose gel stained with ethidium bromide. Both the linearized

plasmids were then excised out from the gel and purified through phenol-chloroform. The linearized plasmids were then transfected into normal HeLa cells by using FuGENE6 (Promega, USA) according to manufacturer's instructions. Transformants were then selected by adding 1 mg/mL of selection marker neomycin in the culture medium. Individual colonies were selected and characterized. Both cells were maintained in Dulbecco's modified Eagle's medium (DMEM) supplemented with 10% heat-inactivated fetal bovine serum (100 U/mL; Nacalai Tesque, Japan) and antibiotics penicillin-streptomycin (100 μg/mL; Nacalai Tesque, Japan), and incubated at 37°C.

4.3   Live cell imaging and immunofluorescence analysis

For the immunofluorescence experiments, cells were either plated in 8-well glass chamber or 12-well plate. After subjected to various treatments such as transfection or viral infection, cells were fixed with 4% of paraformaldehyde (PFA) at RT for 10 min, followed by permeabilization with acetone-methanol (1:1) for 1 min at RT, and blocked with 5 mg/mL in PBST containing 0.1% Tween 20 for 1 h at 4°C. Primary antibodies were added into the samples and incubated at 4°C for overnight. The cells were then incubated by fluorophore-conjugated secondary antibodies (Invitrogen) at 4°C for 1 h. Cells were then washed and nuclei were stained with 4,6-dimaidino-2-phenylinodole (DAPI) for 5 min at RT. The samples were mounted and analysed with the microscope Leica CTR 6500.

For live-cell imaging experiment, HeLa cells stably expressing green fluorescence tagged-G3BP1 plated in 12-well plates were infected with various types of RNA and DNA viruses. After 1 h post-infection, medium containing viruses was removed and 1.0 mL of phenol red free DMEM imaging medium was added. Samples were set into the microscope stage at temperature pre-set to 37°C, supplemented with 5% of carbon dioxide in a humidity-controlled chamber. Imaging was initiated immediately with images captured every 10 min. All live-cell imaging experiments were performed by using Leica model CTR 6500.

4.4   Plaque assay

Both HeLa cells stably expressing EGFP-G3BP1 wild-type and Q325E mutant were infected with EMCV at a specific time point. The cell supernatant was collected and serial dilution was performed. These diluted supernatants were then added to L929 cells and incubated at 37°C for one hour. Supernatants containing viruses were removed and 0.5 mL of 1% agar in 2XMEM was added immediately, and incubated at RT until all agarose was confirmed hardened. The plates were then incubated at 37°C for overnight for plaques to grow. On the next day, 0.5 mL of 0.02% neutral red solution was added to each well and incubated at 37C for 2h. The neutral red solution was removed and the plaques were calculated.

4.5   Enzyme-linked immunosorbent assay (ELISA)

Supernatant of infected cells were collected and subjected to ELISA analysis using kit specifically for human interferon-β (Toray, Japan). All procedures were performed according to the manufacturer's instructions.

4.6   RNA analysis

All RNA in these studies was harvested from cells using TRIzol (Invitrogen) by following the protocols recommended by the manufacturer. Samples were then treated with recombinant DNase I (10 units/μL, Roche) to remove the DNA. Samples were further purified through phenol-chloroform extraction. Concentration of purified RNA was quantified and the quality was examined on agarose stained with ethidium bromide. cDNA was then synthesized by using High Capacity cDNA reverse transcription kit (Applied Biosystems), following the protocols as recommended by manufacturer. cDNA samples were then subjected to either standard PCR reaction or real-time qPCR analysis. Primers used for standard PCR or real-time qPCR involving SYBR system (Applied Biosystem) were all customized and purchased from Invitrogen. Specific probes being used for TaqMan gene expression assay were purchased from Applied Biosystem.

For siRNA analysis, the siRNA universal negative control, siG3BP1and siPKRs were purchased from Invitrogen. These siRNAs were transfected into the cells by

using either RNAiMax or Lipofectamine2000 (Invitrogen) by following manufacturer's instructions. After 48 h post-transfection, cells were subjected to various treatments such as virus infection or PolyI:C transfection. The sequences for the siRNAs and shRNAs are as follows (#*n*, designated siRNA number):

Sense (RIG-I):

5'-CGGAUUAGCGACAAAUUUAUU-3'

Anti-sense (RIG-I):

5'-UAAAUUUGUCGCUAAUCCGUU-3'

Sense (PKR#1):

5'-UUUACUUCACGCUCCGCCUUCUCGU-3'

Anti-sense (PKR#1):

5'-ACGAGAAGGCGGAGCGUGAAGUAAA-3'

Sense (PKR#2):

5'-AUGUCAGGAAGGUCAAAUCUGG-3'

Anti-sense (PKR#2):

5'-CACCCAGAUUUGACCUUCCUGACAU-3'

Sense (G3BP1):

5'-UAAUUUCCCACCACUGUUAAUGCGC-3'

Anti-sense (G3BP1):

5'-GCGCAUUAACAGUGGUGGGAAAUUA-3'

4.7 Immunoblotting analysis

For protein analysis, cells were harvested in ice-cold PBS and subjected to centrifugation to precipitate the lysates. PBS was removed and 100 μL of ice-cold NP-40 lysis buffer containing 1mM of leupeptin, 1 nM of vanadate and phenylmethanesulfonyl fluoride was added. Lysates were completely re-suspended and subjected to centrifugation at 15,000 rpm for 10 min and ultracentrifugation at 100,000 rpm for 5 min. The supernatant was recovered and concentration of protein was quantified through Bradford assay. After boiling for 5 min, protein lysates were separated by SDS-PAGE and transferred onto a nitrocellulose membrane. The membranes were then blocked with 5% skim milk at RT for 30 min, followed by incubation with primary antibody at 4°C overnight. Membranes were washed with TBST and incubated with secondary antibody at 4°C for 1 h. The proteins were visualized through colour development involving alkaline phosphatase buffer and the substrate Nitro Blue Tetrazolium (NBT) (Promega).

4.8 Antibodies

The RIG-I antibodies were made by immunizing a rabbit with a synthetic peptide corresponding to the region 793-807 of RIG-I. Anti-EMCV polyclonal antibody was generated after immunizing a rabbit with purified EMCV viral particles, while anti-MDA5 polyclonal antibodies were generated after immunizing a rat with recombinant MDA5 proteins, which has been preactivated with double-

stranded RNAs. Other antibodies used in these analyses include rabbit monoclonal anti-phospho-PKR pT446 (1:1000) (Epitomics Inc.), rabbit polyclonal anti-PKR (1:1000) (sc-709; Santa Cruz), mouse monoclonal anti-G3BP1 (1:1000) (sc-365338; Santa Cruz), goat polyclonal anti-G3BP1 (1:500) (sc-70283; Santa Cruz), mouse monoclonal anti-GFP (1:500) (MBL), mouse monoclonal anti-FLAG (1:1000) (Sigma-Aldrich), rabbit monoclonal anti-actin (1:5000) (Poly6221; BioLegend), mouse monoclonal anti-poly(A) binding protein (PABP) (1:1000) (ab6125; Abcam), propidium iodide (PI) (1:2000 fold dilution in PBST) (Miltenyi Biotec), rabbit polyclonal anti-HuR (1:1000) (sc-365816; Santa Cruz), goat polyclonal anti-TIAR (1:1000) (sc-1749; Santa Cruz), and the rabbit polyclonal anti-TIA-1/R (1:1000) (sc-48371; Santa Cruz).

4.9   Quantification for the re-distribution pattern of virus induced stress-granule

Quantification of stress granule distribution pattern was performed visually by using eyesight counting. Video media files of live-cell imaging were continuously played back on the computer and total number of cells displaying each unique pattern was recorded manually, and the percentage for each pattern was calculated. As for the quantification of the fixed cells, ten different locations within a sample were chosen randomly. Total number of cells forming SG was calculated and graphs were plotted in percentage.

REFERENCE

Akira, S., Uematsu, S. & Takeuchi, O. 2006. Pathogen recognition and innate immunity. *Cell* **124**, pg. 783-801.

Anderson, P. & Kedersha, N. 2003. Stressful initiations. *Journal of Cell Science* **115**, pg. 3227-3234.

Balachandran, S., Thomas, E. & Barber, G.N. 2004. A FADD-dependent innate immune mechanism in mammalian cells. *Nature* **432**, pg. 401-405.

Barral, P.M., Sarkar, D., Fisher, P.B. & Racaniello, V.R. 2009. RIG-I is cleaved during picornavirus infection. *Virology* **391** (2), pg. 171-176.

Berlanga, J.J., Ventoso, I., Harding, H.P., Deng, J., Ron, D., Sonenberg, N., Carrasco, L. & de Haro C. 2006. Antiviral effect of the mammalian translation initiation factor 2alpha kinase GCN2 against RNA viruses. *The EMBO journal* **25**, pg. 1730-1740.

Borghese, F. & Michiels, T. 2011. The leader protein of cardioviruses inhibits stress granules assembly. *Journal of Virology* **85**(18), pg. 9614-9622.

Clemens, M.J. & Elia, A. 1997. The double-stranded RNA-dependent protein kinase PKR: structure and function. *Journal of Interferon & Cytokine Research* **17**, pg. 503-524.

Der, S.D., Zhou, A., Williams, B.R. & Silverman, R.H. 1998. Identification of genes differentially regulated by interferon alpha, beta, or gamma using oligonucleotide arrays. *Proceedings National Academy of Science, USA* **95**, pg. 15623-15628.

Dougherty, J.D., White, J.P. & Llyod, R.E. 2011. Poliovirus-mediated disruption of cytoplasmic processing bodies. *Journal of Virology* **85**, 64-75.

Emara, M.M. & Brinton, M.A. 2007. Interaction of TIA-1/TIAR with West Nile and dengue virus products in infected cells interferes with stress granule formation and processing body assembly. *Proceedings National Academy of Science, USA* **104**, pg. 9041-9046.

Esclatine, A., Taddeo, B. & Roizman, B. 2004. Herpes simplex virus 1 induces cytoplasmic accumulation of TIA-1/TIAR and both synthesis and cytoplasmic accumulation of tristetraprolin, two cellular proteins that bind and destabilize AU-rich RNAs. *Journal of Virology* **78**, 8582-8592.

Fung, G., Ng. C.S., Zhang, J., Shi, J., Wong, J., Piesik, P., Han, L., Chu, F., Jagdeo, J., Jan, E., Fujita T. & Luo H. 2013. Production of a dominant-negative fragment due to G3BP1 cleavage contributes to the disruption of mitochondria-associated protective stress granules during CVB3 infection. *PLoS ONE* **8**(11), e79546. doi: 10.1371/journal.pone.0079546.

Gale, M. Jr. & Katze, M.G. 1998. Molecular mechanisms of interferon resistance mediated by viral-directed inhibition of PKR, the interferon-induced protein kinase. *Pharmacology & therapeutics* **78**, pg. 29-46.

Gilks, N., Kerdersha, N., Ayodele, M., Shen, L., Stoecklin, G., Dember, L.M. & Anderson, P. 2004. Stress granule assembly is mediated by prion-like aggregation of TIA-1. *Molecular Biology of the Cell* **15** (12), pg. 5383-5398.

Grousl, T., Ivanov, P., Frýdlová, I., Vasicová, P., Janda, F., Vojtová, J., Malínská, K., Malcová, I., Nováková, L., Janosková, D., Valásek, L. & Hasek, J. 2009. Robust heat shock induces eIF2alpha-phosphorylation-independent assembly of stress granule containing eIF3 and 40S ribosomal subunits in budding yeast, Saccharomyces cerevisae. *Journal of Cell Science* **122**, pg. 2078-2088.

Kato, H., Sato. S., Yoneyama, M., Yamamoto, M., Uematsu, S., Matsui, K., Tsujimura, T., Takeda, T., Fujita, T., Takeuchi, O. & Akira, S. 2005. Cell type-specific involvement of RIG-I in antiviral response. *Immunity* **23**, pg. 19-28.

Kato, H., Takeuchi, O., Sato, S., Yoneyama, M., Yamamoto, M., Matsui, K., Uematsu, S., Jung, A., Kawai, T., Ishii, K.J., Yamaguchi, O., Otsu, K., Tsujimura, T., Koh, C.S., Reis e Sousa C., Matsuura, Y., Fujita, T. & Akira, S. 2006. Differential roles of MDA5 and RIG-I helicases in the recognition of RNA viruses. *Nature* **441**, pg. 101-105.

Hoyle, N.P., Castelli, L.M., Campbell, S.G., Holmes, L.E. & Ashe, M.P. 2007. Stress-dependent relocalization of translationally primed mRNPs to cytoplasmic granules that are kinetically and spatially distinct from P-bodies. *The Journal of Cell Biology* **179** (1), pg. 65-74.

Ishikawa, H. & Barber, G.N. 2008. STING is an endoplasmic reticulum adaptor that facilitates innate immune signalling. *Nature* **455**, pg. 674-678.

Iseni, F., Garcin, D., Nishio, M., Kedersha, N., Anderson, P. & Kolakofsky, D. 2002. Sendai virus trailer RNA binds TIAR, a cellular protein involved in virus-induced apoptosis. *The EMBO Journal* **21**, pg. 5141-5150.

Janeway, C.A., Jr. 1989. Approaching the asymptote? Evolution and revolution in immunology. *Cold Spring Harbor Symposia on Quantitative Biology* **54**, pg. 1-13.

Jin, L., Waterman, P.M., Jonscher, K.R., Short, C.M., Reisdorph, N.A. & Cambier, J.C. 2008. MPYS, a novel membrane tetraspanner, is associated with major histocompatibility complex class II and mediates transduction of apoptotic signals. *Molecular and Cellular Biology* **28** (16), pg. 5014-5026.

Jones, C.T., Catanese, M.T., Law, L.M., Khetani, S.R., Syder, A.J., Ploss, A., Oh, T.S., Schoggins, J.W., MacDonald, M.R., Bhatia, S.N. & Rice, C.M. 2010. Real-time imaging of hepatitis C virus infection using a fluorescent cell-based reporter system. *Nature Biotechnology* **28** (2), pg. 167-171.

Kalvakolanu, D.V., Bandyopadhyay, S.K., Harter, M.L. & Sen, G.C. 1991. Inhibition of interferon-inducible gene expression by adenovirus E1A proteins: block in transcriptional complex formation. *Proceedings National Academy of Sciences, USA* **88**, pg. 7459-7463.

Kawai, T., Takahashi, K., Sato, S., Coban, C., Kumar, H., Kato, H., Ishii, K.J., Takeuchi, O. & Akira, S. 2005. IPS-1, an adaptor triggering RIG-I- and Mda5-mediated type I interferon induction. *Nature Immunology* **6** (10), pg. 981-988.

Kawai, T. & Akira, S. 2009. The roles of TLRs, RLRs and NLRs in pathogen recognition. *International Immunology* **21** (4), pg. 317-337.

Kawai, T. & Akira, S. 2010. The role of pattern-recognition receptors in innate immunity: update on Toll-like receptors. *Nature Immunology* **11** (5), pg. 373-384.

Kedersha, N., Cho, M.R., Li, W., Yacono, P.W., Chen, S., Gilks, N., Golan, D.E. & Anderson, P. 2000. Dynamic shuttling of TIA-1 accompanies the recruitment of mRNA to mammalian stress granules. *The Journal of Cell Biology* **151** (6), pg. 1257-1268.

Kedersha, N., Tisdale, S., Hickman, T. & Anderson, P. 2008. Real-Time and Quantitative Imaging of Mammalian Stress Granules and Processing Bodies. *Methods in Enzymology* **448**, pg. 521-552.

Kedersha, N., Gupta, M., Li, W., Miller, I. & Anderson, P. 1998. RNA-binding proteins TIA-1 and TIAR link the phosphorylation of eIF-2 alpha to the assembly of mammalian stress granule. *The Journal of Cell Biology* **147**, pg. 1431-1442.

Kharraz, Y., Salmand, P.A., Camus, A., Auriol, J., Gueydan, C., Kruys, V. & Morello, D. 2010. Impaired Embryonic Development in Mice Overexpressing the RNA-Binding Protein TIAR. *PLoS ONE* **5**(6), e11352.

Langereis, M.A., Feng, Q. and van Kuppeveld F.J. 2013. MDA5 localizes to stress granules but this localization is not required for the induction of type I interferon. *Journal of Virology* **87**(11), pg. 6314-6325.

Li, W., Li, Y., Kedersha, N., Anderson, P., Emara, M., Swiderek, K.M., Moreno, G.T. & Brinton, M.A. 2002. Cell proteins TIA-1 and TIAR interact with the 3' stem-loop of the West Nile virus complementary minus-strand RNA and facilitate virus replication. *Journal of Virology* **76**, pg. 11989-12000.

López de Silanes, I., Galbán, S., Martindale, J.L., Yang, X., Mazan-Mamczarz, K., Indig, F.E., Falco, G., Zhan, M. & Gorospe, M. 2005. Identification and functional outcome of mRNAs associated with RNA-binding protein TIA-1. *Molecullar and Cellular Biology* **25** (21), pg. 9520-9531.

Meylan, E., Curran, J., Hofmann, K., Moradpour, D., Binder, M., Bartenschlager, R. & Tschopp, J. 2005. Cardif is an adaptor protein in the RIG-I antiviral pathway and is targeted by hepatitis C virus. *Nature* **437**, pg. 1167-1172.

Michallet, M.C., Meylan, E., Ermolaeva, M.A., Vazquez, J., Rebsamen, M., Curran, J., Poeck, H., Bscheider, M., Hartmann, G., König, M., Kalinke, U., Pasparakis, M. & Tschopp, J. 2008. TRADD protein is essential component of the RIG-like helicase antiviral pathway. *Immunity* **28**, pg. 651-661.

Nallagatla, S.R., Hwang, J., Toroney, R., Zheng, X., Cameron, C.E., Bevilacqua, P.C. 2007. 5'-triphosphate-dependent activation of PKR by RNAs with short stem-loops. *Science* **318** (5855), pg. 1455-1458.

Onoguchi, K., Onomoto, K., Takamatsu, S., Jogi, M., Takemura, A., Morimoto, S., Julkunen, I., Namiki, H., Yoneyama, M. & Fujita, T. 2010. Virus-infection or 5'ppp-RNA activates antiviral signal through redistribution of IPS-1 mediated by MFN1. *PLoS Pathogen* **6** (7), e1001012.

Onomoto, K., Jogi, M., Yoo J.S., Narita R., Morimoto S., Takemura A., Sambhara S., Kawaguchi A., Osari S., Nagata K., Matsumiya T., Namiki H., Yoneyama M. *&* Fujita, T. 2012. Critical role of an antiviral stress granule containing RIG-I and PKR in viral detection and innate immunity. *PLoS ONE* 7:e43031.

Pesch, V.V., Eyll, O.V. & Michiels, T. 2001. The leader protein of Theiler's Virus Inhibits Immediate-early Alpha/Beta Interferon Production. *Journal of Virology* **75**(17), pg. 7811-7817.

Pichlmair. A., Schulz, O., Tan, CP., Rehwinkel, J., Kato, H., Takeuchi, O., Akira, S., Way, M., Schiavo, G. & Reis e Sousa C. 2009. Activation of MDA5 requires higher-order RNA structures generated during virus infection. *Journal of Virology* **83**, pg. 10761-10769.

Qin, Q., Hastings, C. & Miller, C.L. 2009. Mammalian orthoreovirus particles induce and are recruited into stress granules at early times postinfection. *Journal of Virology* **83**, pg. 11090-11101.

Reich, N., Pine, R., Levy, D. & Darnell, J.E. Jr. 1988. Transcription of interferon-stimulated genes is induced by adenovirus particles but is suppressed by E1A gene products. *Journal of Virology* **62**, pg. 114-119.

Ruggieri, A., Dazert, E., Metz, P., Hofmann, S., Bergeest, J.P., Mazur, J., Bankhead, P., Hiet, M.S., Kallis, S., Alvisi, G., Samuel C.E., Lohmann, V., Kaderali, L., Rohr, K., Frese, M. Stoecklin, G. & Bartenschlager, R. 2012. Dynamic oscillation of translation and stress granule formation mark the cellular response to virus infection. *Cell Host Microbe* **12**, pg. 71-85.

Saha, S.K., Pietras, E.M., He, J.Q., Kang, J.R., Liu, S.Y., Oganesyan, G., Shahangian, A., Zarnegar, B., Shiba, T.L., Wang, Y. & Cheng, G. 2006. Regulation of antiviral responses by a direct and specific interaction between TRAF3 and Cardif. *EMBO Journal* **25** (14), pg. 3257-3263.

Seth, R.B., Sun, L., Ea, C.K. & Chen, Z.J. 2005. Identification and characterization of MAVS, a mitochondrial anti-viral signaling protein that activates NF-kappaB and IRF3. *Cell* **122**, pg. 669-682.

Simpson-Holley, M., Kedersha, N., Dower, K., Rubins, K.H., Anderson, P., Hensley, L.E. & Connor, J.H. 2011. Formation of antiviral cytoplasmic granules during Orthopoxvirus infection. *Journal of Virology* **85**, pg. 1581-1593.

Sun, W., Li, Y., Chen, L., Chen, H., You, F., Zhou, X., Zhou, Y., Zhai, Z., Chen, D. & Jiang, Z. 2009. ERIS, an endoplasmic reticulum IFN stimulator, activates innate immune signaling through dimerization. *Proceedings of the National Academy of Sciences, USA* **106** (21), pg. 8653-8658.

Takahasi, K., Yoneyama, M., Nishihori, T., Hirai, R., Kumeta, H., Narita, R., Gale, M., Inagaki, F. & Fujita, T. 2008. Nonself RNA-Sensing Mechanism of RIG-I Helicase and Activation of Antiviral Immune Responses. *Molecular Cell* **29**, pg. 428-440.

Thomas, M.G., Loschi, M., Desbats, M.A. & Boccaccio, G.L. 2011. RNA granules: the good, the bad and the ugly. *Cell Signaling* **23** (2), pg. 324-334.

Tourrière, H., Chebli, K., Zekri, L., Courselaud, B., Blanchard, J.M., Bertrand, E. & Tazi, J. 2003. The RasGAP-associated endoribonuclease G3BP assembles stress granules. *The Journal of Cell Biology* **160** (6), pg. 823-831.

White, J.P., Cardenas, A.M., Marissen, W.E. & Lloyd, R.E. 2007. Inhibition of cytoplasmic mRNA stress granule formation by a viral proteinase. *Cell Host & Microbe* **2** (5), pg. 295-305.

Wylie, K.M., Schrimpf, J.E. & Morrison LA. 2009. Increased eIF2alpha phosphorylation attenuates replication of herpes simplex virus 2 vhs mutants in mouse embryonic fibroblasts and correlates with reduced accumulation of the PKR antagonist ICP34.5. *Journal of Virology* **83**, pg. 9151-9162.

Xu, L.G., Wang, Y.Y., Han, K.J., Li, L.Y., Zhai, Z. & Shu, H.B. 2005. VISA Is an Adapter Protein Required for Virus-Triggered IFN-beta Signaling. *Molecular Cell* **19**, pg. 727-740.

Yoneyama, M., Kikuchi, M., Natsukawa, T., Shinobu, N., Imaizumi, T., Miyagishi, M., Taira, K., Akira, S. & Fujita, T. 2004. The RNA helicase RIG-I has an essential function in double-stranded RNA-induced innate antiviral responses. *Nature Immunology* **5**, pg. 730-737.

Yoneyama, M., Kikuchi, M, Matsumoto, K., Imaizumi, T., Miyagishi, M., Taira, K., Foy, E., Loo, Y.M., Gale, M., Akira, S., Yonehara, S., Kato, A. & Fujita, T. 2005. Shared and unique functions of the DExD/H-box helicases RIG-I, MDA5, and LGP2 in antiviral innate immunity. *Journal of Immunology* **175** (5) pg, 2851-2858.

Yoneyama, M. & Fujita, T. 2010. Recognition of viral nucleic acids in innate immunity. *Reviews in Medical Virology* **20**, pg. 4-22.

Yoshida, R., Takaesu, G., Yoshida, H., Okamoto, F., Yoshioka, T., Choi, Y., Akira, S., Kawai, T., Yoshimura, A. & Kobayashi, T. 2008. TRAF6 and MEKK1 play a vital role in the RIG-I-like helicase antiviral pathway. *Journal of Biological Chemistry* **283**, pg. 36211-36220.

Zeng, W. & Chen, Z. 2008. MITAgating Viral Infection. *Immunity* **29** (4), pg. 513-515.

Zhong, B., Yang, Y., Li, S., Wang, Y.Y., Li, Y., Diao, F., Lei, C., He, X., Zhang, L., Tien, P. & Shu, H.B. 2008. The Adaptor Protein MITA Links Virus-Sensing Receptors IRF3 Transcription Factor Activation. *Immunity* **29** (4), pg. 538-550.

TABLE

Table 1   Three distinct distribution patterns of vSG after infected by both RNA and DNA viruses.

Virus-induced stress granule distribution pattern	SG component	Viruses
Type I: Stable formation	Ras-GAP SH3-binding protein-1 (G3BP1)	NDV, IAVΔNS1, AdenoWT5, HCV[1]
	T-cell intracellular antigen-1 (TIA-1/R)	NDV, IAVΔNS1
Type II: Transient formation	Ras-GAP SH3-binding protein-1 (G3BP1)	PV[1], EMCV, SINV, HCV[1],
	T-cell intracellular antigen-1 (TIA-1/R)	WNV[1], DV[1], SFV[1], Rotavirus[1], HSV1/2[1], VV[1]
Type III: Alternate formation (*n* times)	Ras-GAP SH3-binding protein-1 (G3BP1)	HCV[1], Adeno5ΔE1A
	T-cell intracellular antigen-1 (TIA-1/R)	No record(s)
No significant numbers of cells form SG	Ras-GAP SH3-binding protein-1 (G3BP1)	SeV, VSV, IAV WT
	T-cell intracellular antigen-1 (TIA-1/R)	SeV, VSV, IAV WT

[1]As noted from existing publications

FIGURES
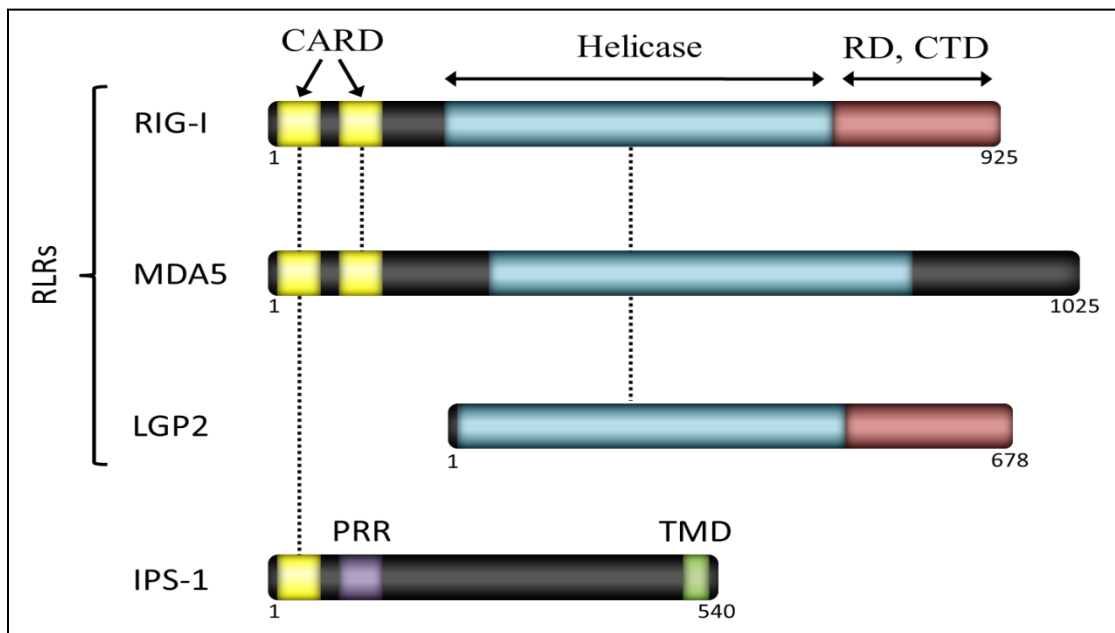
FIG 1.   Schematic model for RLR family members.
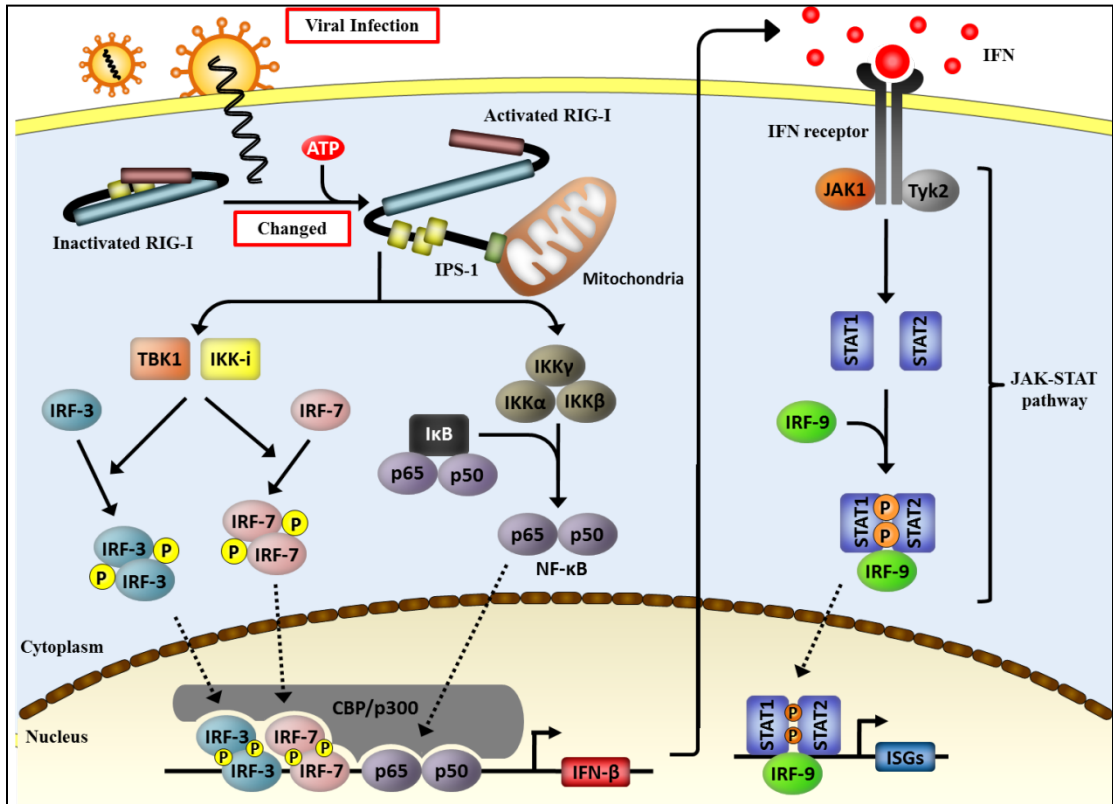
FIG 2.   Schematic diagram of RLR-mediated interferon signalling.
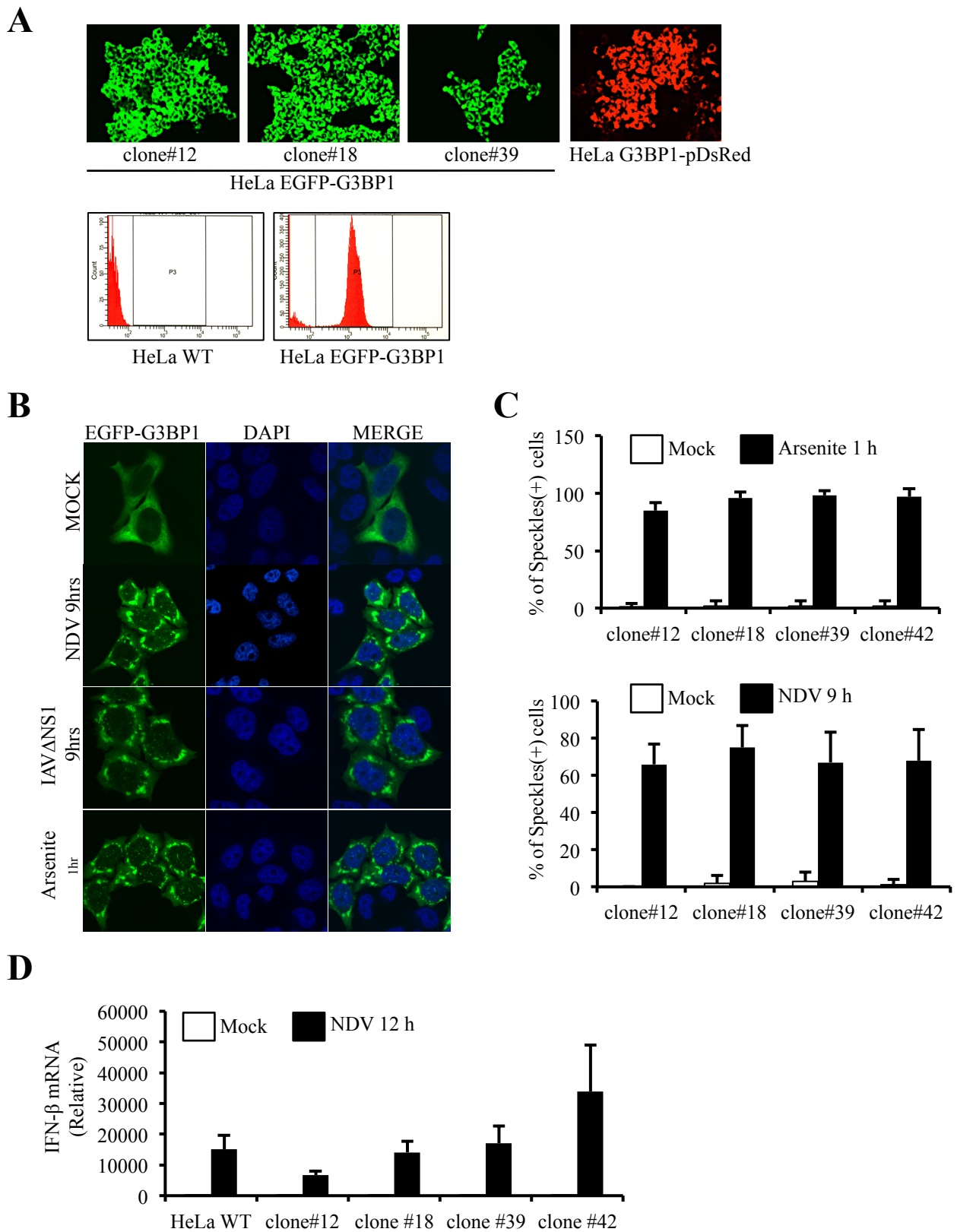
A clone#12 clone#18 clone#39 HeLa EGFP-G3BP1 HeLa G3BP1-pDsRed

HeLa WT HeLa EGFP-G3BP1

B EGFP-G3BP1 DAPI MERGE (MOCK, NDV 9hrs, IAVΔNS1 9hrs, Arsenite 1hr)

C % of Speckles(+) cells (Mock, Arsenite 1 h; Mock, NDV 9 h) clone#12 clone#18 clone#39 clone#42

D IFN-β mRNA (Relative) (Mock, NDV 12 h) HeLa WT, clone#12, clone #18, clone #39, clone #42

FIG 3. Generation and functional characterization of pEGFP-G3BP1 HeLa transduced cells
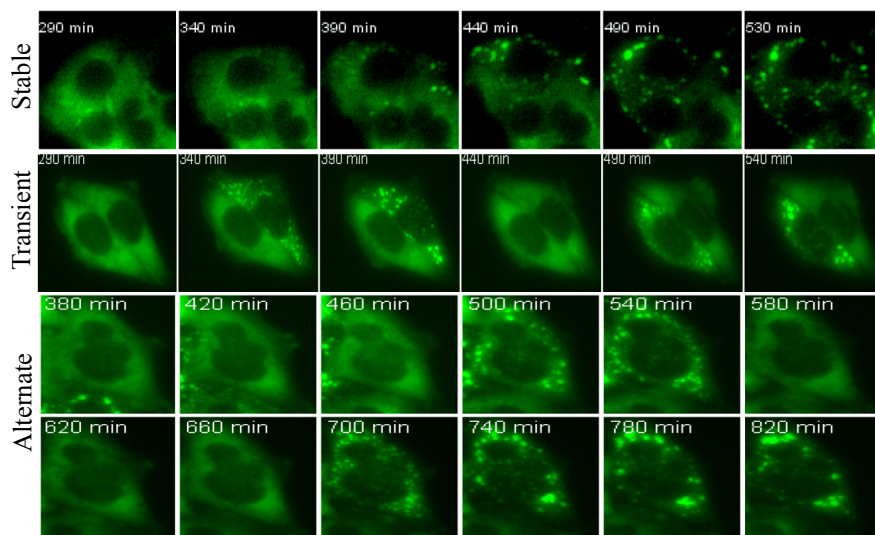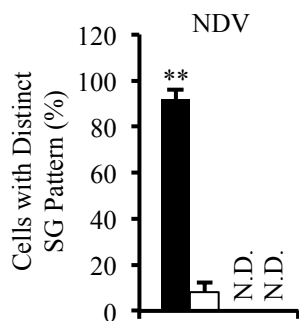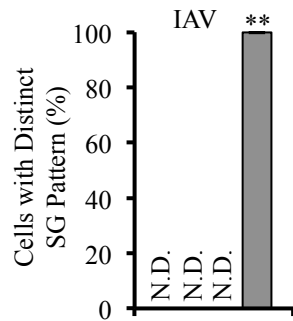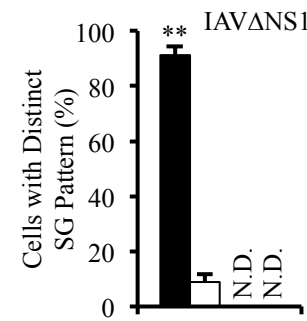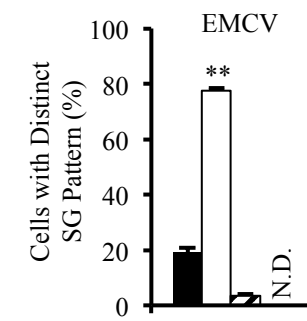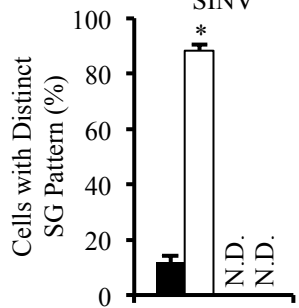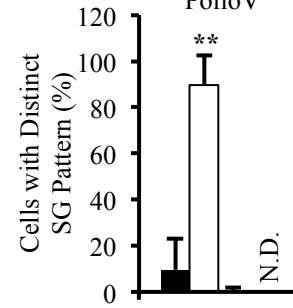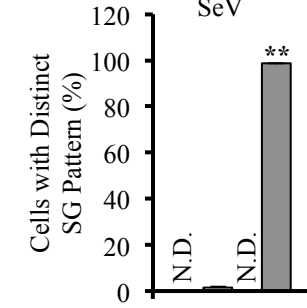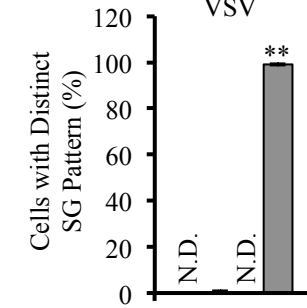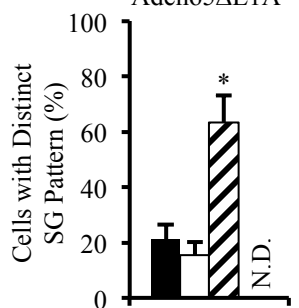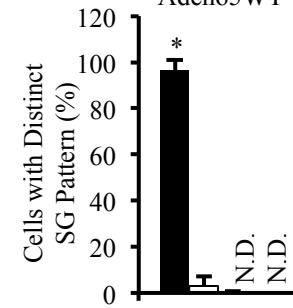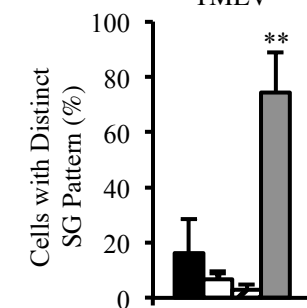
FIG 4. RNA and DNA viruses induce four distinct patterns of stress granules redistribution

53

A

IB: α-GFP

MW (kDa)

N.C. Mock EMCV 0 2 4 6 8 10 p.h.i

116
97

← EGFP-G3BP1 (≈ 96kDa)

← EGFP-G3BP1 cp (≈ 80 kDa)

IB: α-actin

45

β-actin

1 2 3 4 5 6 7 8

IB: α-FLAG

MW (kDa)

N.C. Mock EMCV 0 2 4 6 8 10 p.h.i

66 —

FLAG-G3BP1
Q325E

IB: α-actin

45 —

β-actin

1 2 3 4 5 6 7 8

B

HeLa

pEmpty pLeader p3C EMCV

IB: α-G3BP1

MW (kDa)
95 —
72 —
55 —
43 —
34 —
26 —

Endogenous
G3BP1

G3BP1 cp

IB: α-actin

55 —
43 —

Lane 1 2 3

G/G3BP1 WT   G/G3BP1 Q325E

HeLa WT pEmpty pLeader p3C EMCV pEmpty pLeader p3C EMCV

IB: α-GFP

MW (kDa)
95 —
72 —
55 —

EGFP-G3BP1

G3BP1 cp

IB: α-actin

55 —
43 —

β-actin

Lane 1 2 3 4 5 6 7

FIG 5. Cleavage of G3BP1 results in transient formation of SG after EMCV infection

54

A

EMCV

0 8 12 p.h.i

◄ EGFP-G3BP1

◄ Endogenous
   G3BP1

IB: α-G3BP1
    (C-14)

◄ G3BP1 cp

IB: α-actin   β-actin

1 2 3

B

NTF2-like ─ Acidic ─■─ RRM ─ RGG

PxxP

EMCV 3C^PRO

FIG 6. EMCV 3C protease targets C-terminal region of G3BP1

A

EGFP-G3BP1

B

EGFP-G3BP1 Q325E

C

FIG 7. HeLa EGFP-G3BP1 Q325E mutant transduced cells show persistent formation of SG.

FIG 8. Other SG components are not cleaved after EMCV infection.
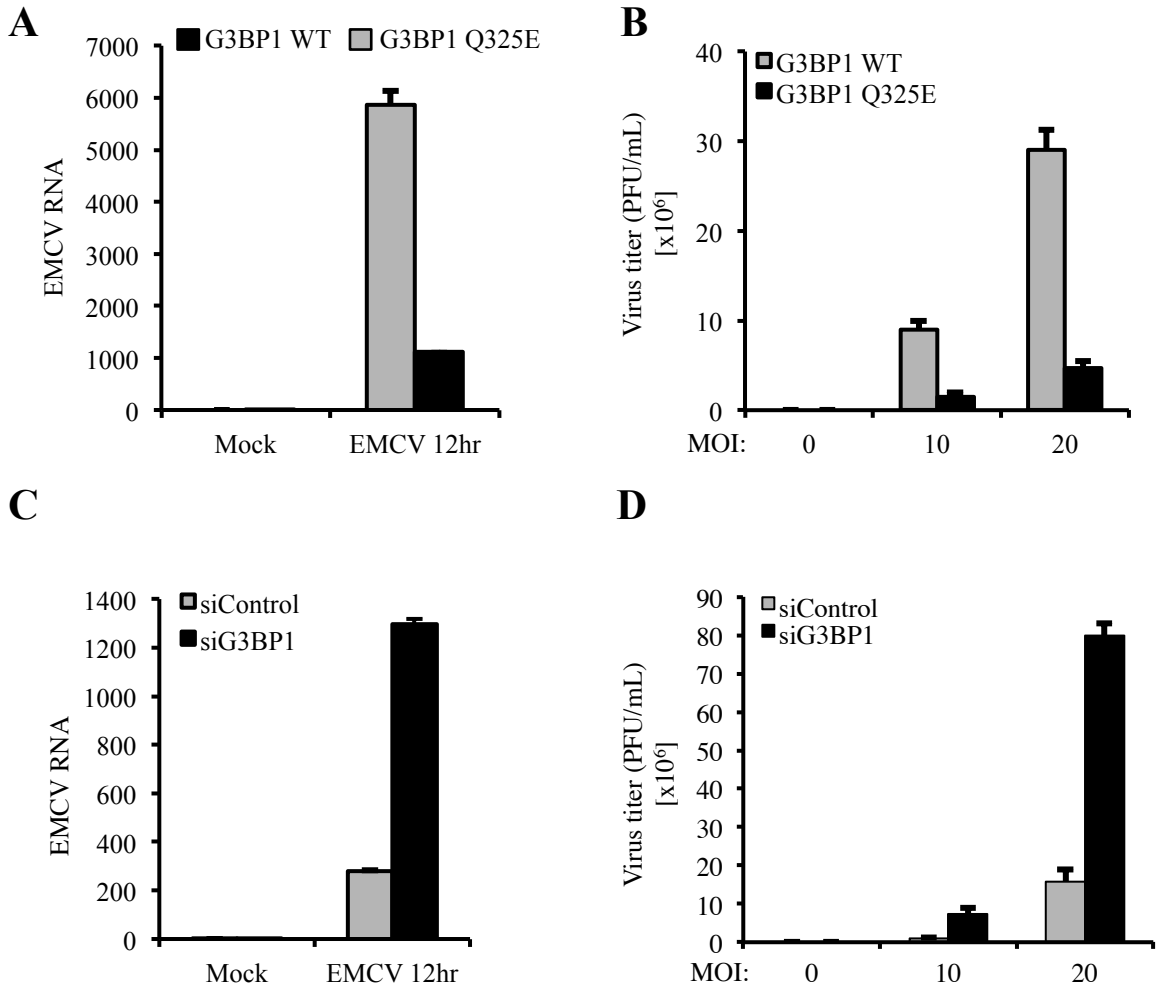
FIG 9. Dispersion of SG due to cleavage of G3BP1 potentiates EMCV replication.
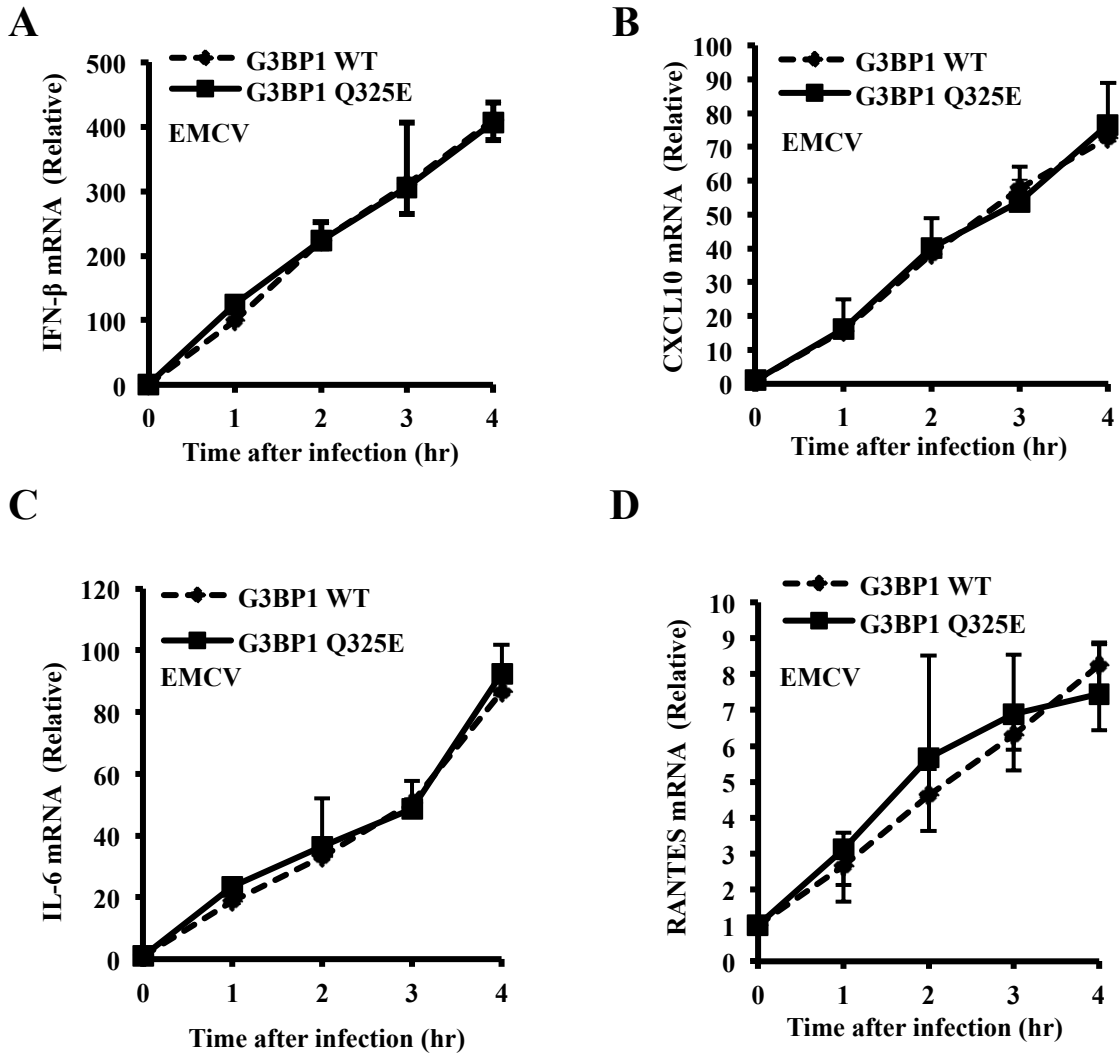
FIG 10. IFN-β and other chemokine genes expression were not affected at the early phase in both G3BP1 WT and Q325E mutant cells.
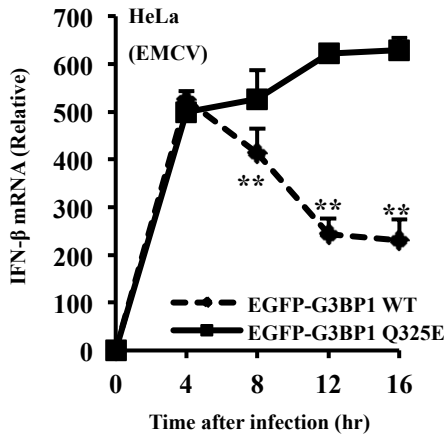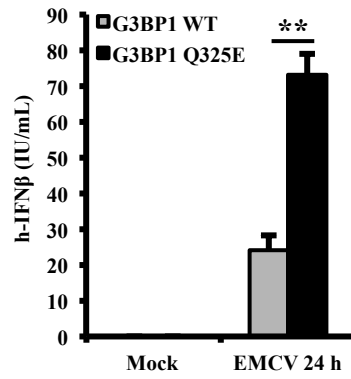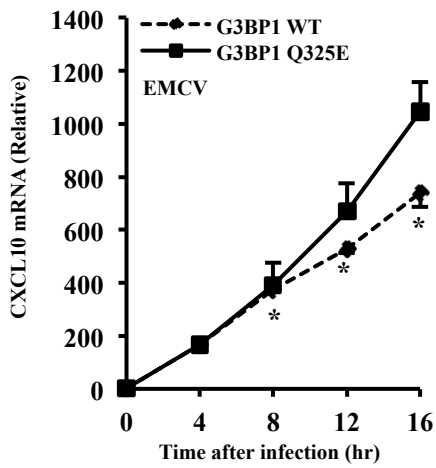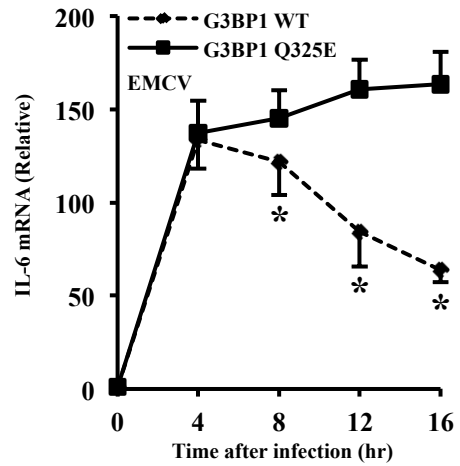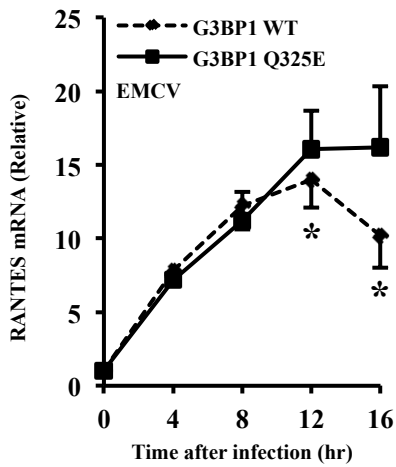
FIG 11. Cleavage of G3BP1 impaired the IFN-β production and the activation other chemokine genes after EMCV infection.
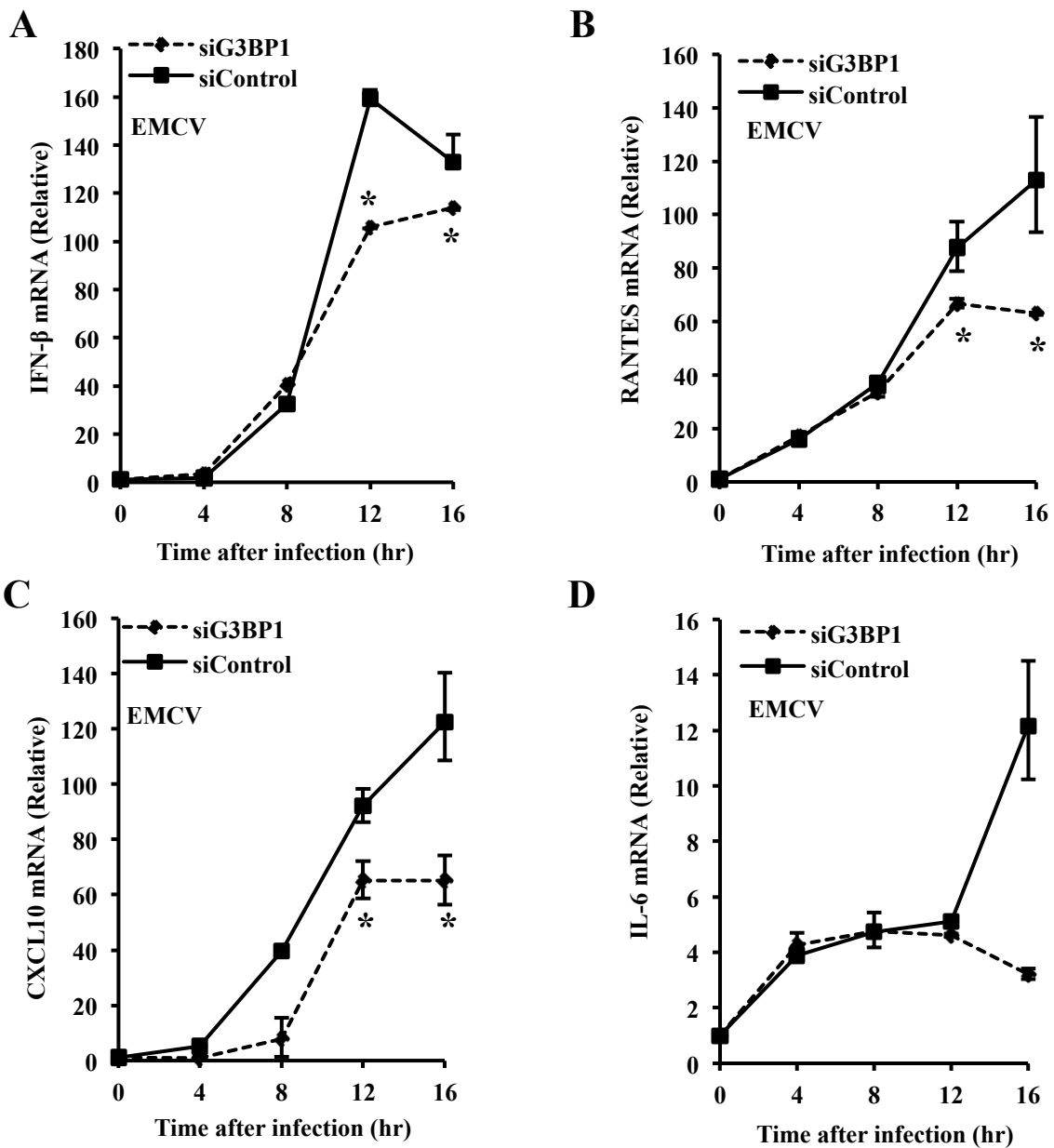
FIG 12. Endogenous depletion of G3BP1 attenuated the activation of IFN-β and chemokine genes expression after EMCV infection.
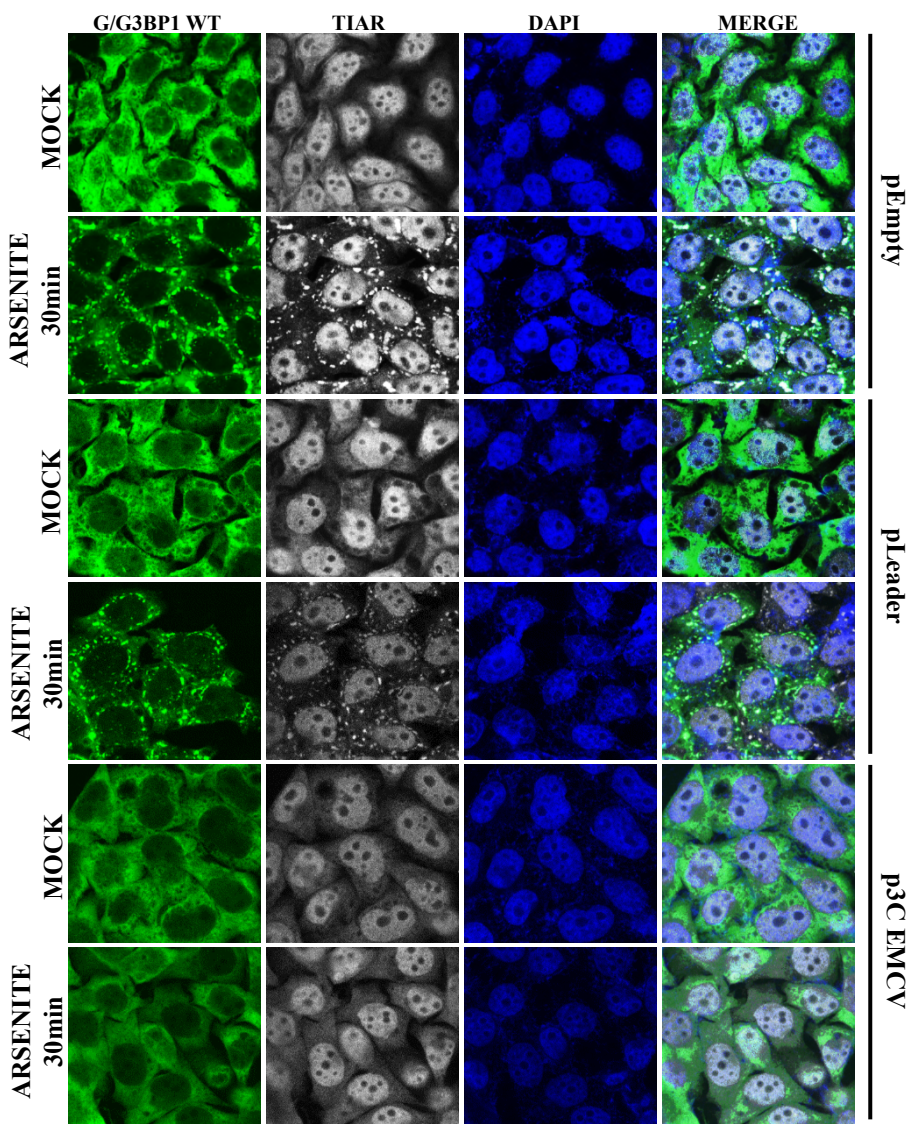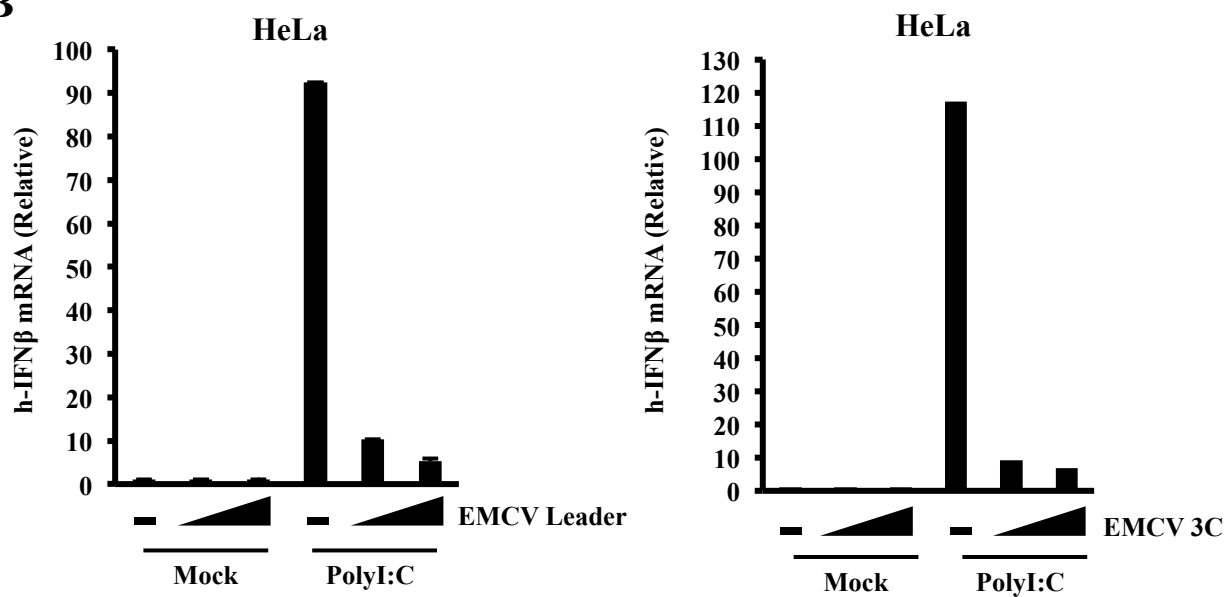
FIG 13. EMCV 3C, but not leader protein inhibits SG-dependent IFN-β production.
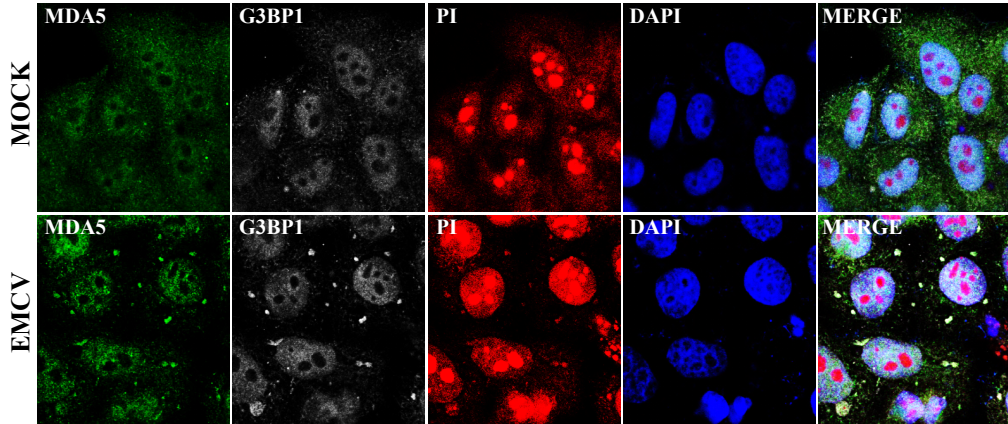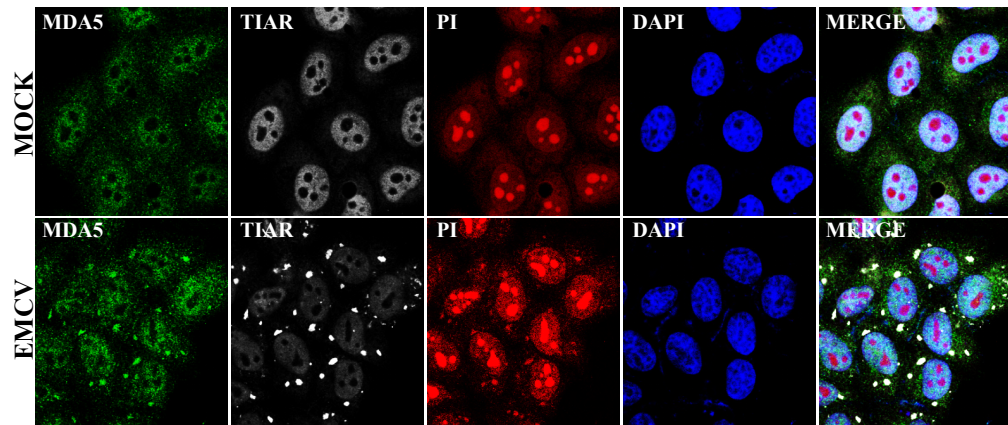
FIG 14. MDA5 are co-localized with SG components after EMCV infection

A
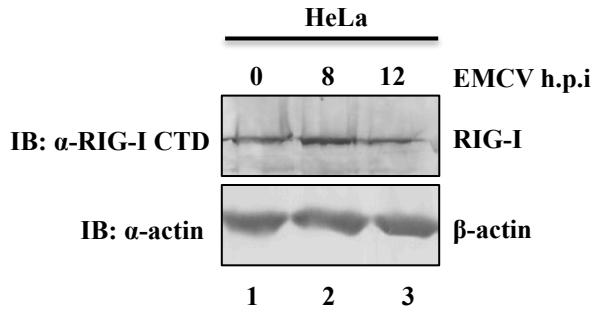
B
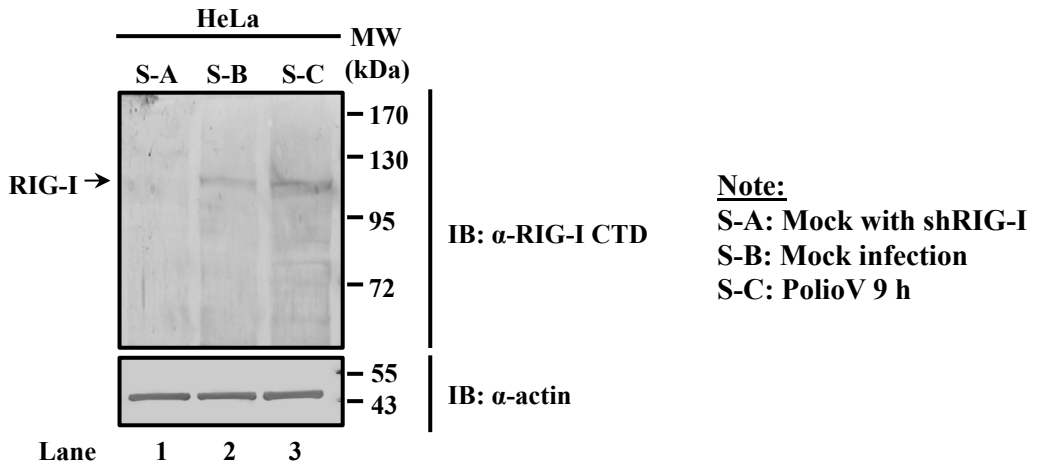
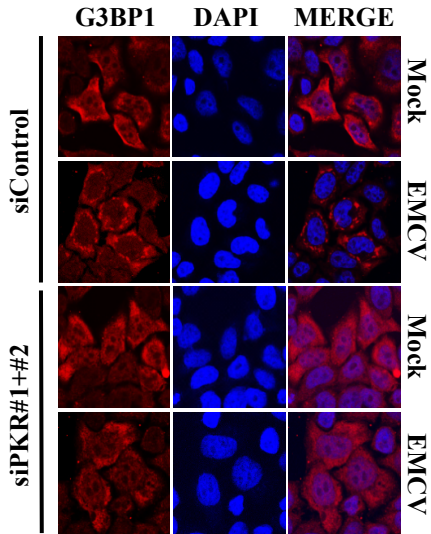FIG 15. RIG-I expression remains intact after EMCV and PolioV infection.
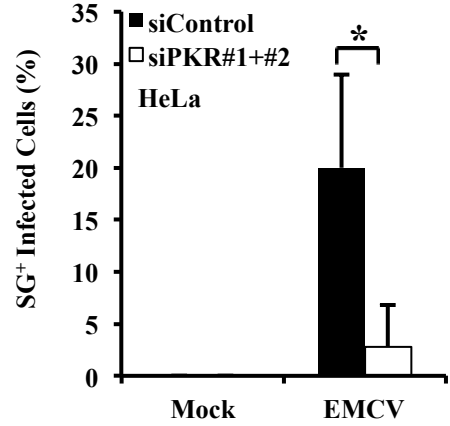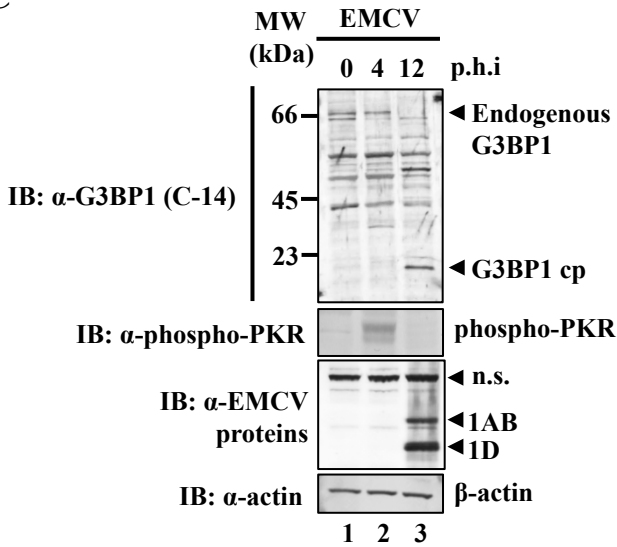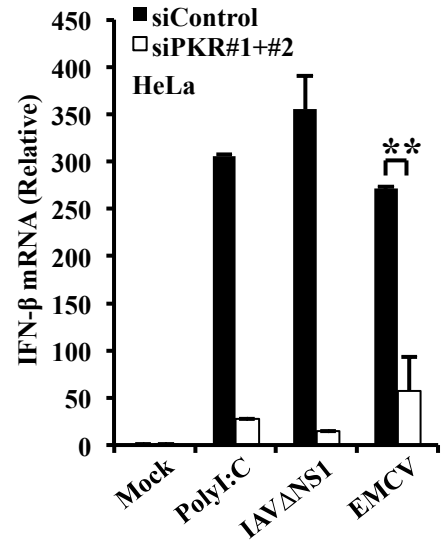
A

B

C

D

FIG 16. PKR is critical for EMCV-induced SG and IFN-β gene activation

TABLE LEGENDS

Table No.

1.0   Three distinct distribution patterns of vSG after infected by both RNA and DNA viruses.

Figure No.

1.   **Schematic model for RLR family members.**

RIG-I, MDA-5 and LGP2 share a typical DEAD box helicase domain containing ATPase activity, which is essential for the binding of dsRNA. At the N-terminal region, both RIG-I and MDA-5 possess CARDs, which will bind to the CARD found in the N-terminal region of their signalling adaptor, IPS-1, through homotypic interaction. CARD is found in LGP2. The RD region located within the C-terminal domain of RIG-I and LGP2 are involved in autoregulation.

2.   **Schematic diagram of RLR-mediated interferon signalling.**

Under uninfected state, inactive RIG-I will remain in a closed conformation. After viral infection, engagement of RIG-I with the viral 5'ppp and dsRNA will trigger its conformation changed, exposing its CARD domain to form the CARD-CARD homotypic interaction with IPS-1, followed by the recruitment of other signalling components to form a large "signalosome" complexes and eventually produce IFN. Secreted mature IFN proteins will bind with its receptors and induce the expression of ISGs through JAK-STAT pathway.

3.   **Generation and functional characterization of pEGFP-G3BP1 HeLa transduced cells.**

(A) Four independent clones of HeLa EGFP-G3BP1 were screened out and examined for expression by using confocal microscope and FACS sorting.

(B) HeLa EGFP-G3BP1 clone#12 was either mock treated, or stimulated with indicated viruses or arsenite. Cells were fixed with 4% PFA and stress granule formation was examined by using confocal miscroscope.

(C) Four independent clones of HeLa EGFP-G3BP1 transduced cells were either arsenite treated for 1 h, or infected with NDV for 9 h. Cells were fixed and the percentage of cells with SG formation were quantified.

(D) HeLa wild-type and HeLa EGFP-G3BP1 transduced cells were infected with NDV for 12 h. RNA was harvested and the expression of IFN-β mRNA was quantified.

(All error bars indicate ±S.D. of duplicates)

4. RNA and DNA viruses induce three distinct patterns of stress granule redistribution.

(A) Representative montage of images for classification of stable formation, transient formation, and alternate SG formation.

(B-L) HeLa EGFP-G3BP1 stable cells were infected with NDV, IAV, IAVΔNS1, EMCV, SINV, PolioV, SeV, VSV, Adeno5ΔE1A, Adeno5WT, and TMEV for 1 h. Imaging was initiated immediately and percentage of cells with distinct SG formation patterns were quantified.

(Error bars represents the ±S.D. n=3; N.D.=non-detected; **P<0.005; *P<0.05)

5. Cleavage of G3BP1 results in transient formation of SG after EMCV infection.

(A) HeLa EGFP-G3BP1 (*upper*) and FLAG-G3BP1 Q325E mutant (*lower*) stable cells were infected by EMCV (MOI: 10) and protein was harvested at different indicated time point. Western blot analysis was performed to analyze the cleavage with indicated antibodies.

(B) (*Left*) HeLa cells were transfected with an empty vector, expression vector for EMCV leader, or 3C protease. After 48 h of incubation, protein was harvested and analyzed for endogenous G3BP1 cleavage through immunoblotting. (*Right)* Empty vector and expression vector for EMCV 3C and leader protein were transfected into HeLa EGFP-G3BP1 WT and Q325E mutant stable cells. After 48 h of incubation, protein was harvested and the cleavage of G3BP1 was analyzed through immunoblotting.

6. EMCV 3C protease targets C-terminal region of G3BP1.

(A) HeLa cells were mock treated or infected with EMCV (MOI:10). Protein was harvested at the different indicated time point. Western blot was performed with antibody specifically targeting C-terminal portion of G3BP1.

(B) Schematic diagram of G3BP1 cleavage by EMCV 3C protease.

7.   **HeLa EGFP-G3BP1 Q325E mutant transduced cells show persistent formation of SG.**

(A and B) HeLa EGFP-G3BP1 WT and Q325E mutant stably expressing cells were infected with EMCV (MOI: 10). SG formation was monitored using live-cell imaging. Montage series are the selected representative images captured every 40 min.

(C) Imaging data obtained for HeLa EGFP-G3BP1 Q325 mutant cells (panel B) was further subjected to the quantification analysis for the SG formation pattern. (Error bars represents the ±S.D. for n=3; **P<0.005)

8.   **Other SG components are not cleaved after EMCV infection.**

HeLa EGFP-G3BP1 WT cells were mock treated or infected with EMCV (MOI=10). Cell lysates were harvested at the different indicated time points. Western blot was performed and protein levels of various SG components were analyzed by using specific antibodies.

9.   **Dispersion of SGs due to cleavage of G3BP1 potentiates EMCV replication.**

(A) Both HeLa EGFP-G3BP1 WT and Q325E mutant stably expressing cells were mock treated or infected with EMCV (MOI: 10). Total RNA was harvested and purified. EMCV RNA was quantified using RT-qPCR.

(B) Both HeLa EGFP-G3BP1 WT and Q325E stably expressing cells were either mock treat or infected with EMCV at two different MOIs (MOI=10 or MOI=20). Culture medium containing viruses were collected and subjected to plaque assay to examine the viral titer.

(C) HeLa cells were transfected with control siRNA and siRNA targeting human G3BP1. After incubation for 48 h, cells were mock infected or infected with EMCV (MOI: 10). After 12 h, total RNA was harvested and purified. EMCV RNA was quantified using RT-qPCR.

(D) HeLa cells were transfected with control siRNA and siRNA targeting human G3BP1. After incubation for 48 h, cells were either mock or infected with EMCV at two different MOIs (MOI=10 or MOI=20). Culture medium containing viruses were collected and subjected to plaque assay to examine the viral titer.

(Error bars represents ±S.D. n=2)

10. **IFN-β and other chemokine genes expression were not affected at the early phase in both G3BP1 WT and Q325E mutant cells.**

    Both HeLa EGFP-G3BP1 WT and Q325E mutant stable cells were either mock treated or infected with EMCV (MOI: 10). Total RNA was harvested and purified at indicated time points. Expression level for (A) IFN-β, (B) CXCL 10, (C) 1L-6, and (D) RANTES mRNA was examined.

    (Error bars represents ±S.D. n=2)

11. **Cleavage of G3BP1 impaired the IFN-β production and the activation of other chemokine gene after EMCV infection.**

    (A) Both HeLa EGFP-G3BP1 WT and Q325E mutant stable cells were either mock treated or infected with EMCV (MOI: 10). Total RNA was harvested and purified at indicated time points. Expression level for IFN-β mRNA was examined using RT-qPCR approach.

    (B) Both HeLa EGFP-G3BP1 WT and Q325E mutant stable cells were either mock treated or infected with EMCV (MOI: 10). After 24 h of incubation, cell culture supernatant was collected and subjected to enzyme-linked immunosorbent assay for human IFN-β.

    (C-E) Both HeLa EGFP-G3BP1 WT and Q325E mutant stable cells were either mock treated or infected with EMCV (MOI: 10). Total RNA was harvested and purified at indicated time points. Expression level for (C) CXCL10, (D) 1L-6, and (E) RANTES mRNA was examined.

    (Error bars represents ±S.D. n=2, **P<0.005, *P<0.05)

12. **Endogenous depletion of G3BP1 attenuated the activation of IFN-β and other chemokine gene expression after EMCV infection.**

    HeLa cells were transfected with control siRNA or siRNA targeting human G3BP1. After incubation for 48 h, cells were either mock or infected with EMCV (MOI=10). Total RNA was harvested and purified at the indicated time points and expression for (A) IFN-β, (B) RANTES, (C) CXCL10, and (D) 1L-6 mRNA was examined by using RT-qPCR approach.

(Error bars represent ±S.D. n=2, *P<0.05)

13.   EMCV 3C, but not leader inhibits SG-dependent IFN-β production.

(A) HeLa EGFP-G3BP1 cells were transfected with empty vector, vector encoding EMCV leader and 3C protease. After 48 h, cells were treated with arsenite for 30 min. Cells were fixed and stained for the indicated protein. Nuclei were stained with DAPI. Images were obtained through confocal microscope.

(B) HeLa cells were transfected with empty vector, expression vector for EMCV leader and 3C protease. After 48 h, cells were either mock or polyI:C transfected. After 12 h, total RNA was harvested and purified. Expression of IFN-β mRNA was examined.

14.   MDA5 are co-localized with SG components after EMCV infection.

HeLa cells were infected with EMCV (MOI=10). Cells were fixed with 4% PFA and both stained for MDA5, PI and (A) G3BP1, (B) TIAR. Nuclei were stained with DAPI. Samples were analyzed by using confocal microscope.

15.   RIG-I expression remains intact EMCV and PolioV infection.

(A) HeLa cells were mock treated or infected with EMCV (MOI=10). Protein lysates were harvested at indicated time points and analyzed for endogenous RIG-I expression.

(B) HeLa cells transfected with short-hairpin RIG-I and HeLa parental cells were either mock treated or infected with PolioV. Protein lysates were harvested and analyzed for endogenous RIG-I cleavage.

16.   PKR is critical for EMCV-induced SG and IFN-β gene activation.

(A) HeLa cells were transfected with control siRNA or siRNAs targeting human PKR. After 48 h of incubation, cells were either mock treated or infected with EMCV (MOI=10) for 6 h. Cells were fixed and stained with indicated proteins. Samples were observed under confocal microscope.

(B) Samples from panel (A) were analyzed for the total number of cells which shows SG formation.

(C) HeLa cells were mock treated or infected with EMCV (MOI=10). Protein

lysates were harvested at indicated time points and were subjected to western blotting analysis by using specific antibodies.

(D) HeLa cells were transfected with control siRNA or siRNA targeting human PKR. After 48 h of incubation, cells were either mock treated or stimulated with indicated treatments. Total RNA was harvested and purified. Expression level of IFN-β mRNA was determined.

($**P<0.005$, $*P<0.05$)

ACKNOWLEDGEMENT

This thesis is based on the material contained in the following scholarly article.

Chen Seng Ng, Michihiko Jogi, Ji-Seung Yoo, Koji Onomoto, Satoshi Koike, Takuya Iwasaki, Mitsutoshi Yoneyama, Hiroki Kato, and Takashi Fujita.

Encephalomyocarditis Virus Disrupts Stress Granules, the Critical Platform for Triggering Antiviral Innate Immune Responses.

Journal of Virology
(September 2013, Volume: 87, Number: 17, pg: 9511-9522; DOI: 10.1128/JVI.03248-12)